

Multitask diffusion adaptation over asynchronous networks

Roula Nassif[†], *Student Member, IEEE*, Cédric Richard[†], *Senior Member, IEEE*

André Ferrari[†], *Member, IEEE*, Ali H. Sayed[‡], *Fellow Member, IEEE*

[†] Laboratoire Lagrange

Université de Nice Sophia-Antipolis, France

phone: (33) 492 076 394 fax: (33) 492 076 321

roula.nassif@oca.eu cedric.richard@unice.fr andre.ferrari@unice.fr

[‡] Electrical Engineering Department

University of California, Los Angeles, USA

phone: (310) 267 2142 fax: (310) 206 8495

sayed@ee.ucla.edu

Abstract

The multitask diffusion LMS is an efficient strategy to simultaneously infer, in a collaborative manner, multiple parameter vectors. Existing works on multitask problems assume that all agents respond to data synchronously. In several applications, agents may not be able to act synchronously because networks can be subject to several sources of uncertainties such as changing topology, random link failures, or agents turning on and off for energy conservation. In this work, we describe a model for the solution of multitask problems over asynchronous networks and carry out a detailed mean and mean-square error analysis. Results show that sufficiently small step-sizes can still ensure both stability and performance. Simulations and illustrative examples are provided to verify the theoretical findings. The framework is applied to a particular application involving spectral sensing.

The work of C. Richard and A. Ferrari was partly supported by ANR and DGA grant ANR-13-ASTR-0030 (ODISSEE project). The work of A. H. Sayed was supported in part by NSF grants CCF-1011918 and ECCS-1407712. A short version of this work appears in the conference publication [1].

I. INTRODUCTION

Distributed adaptive learning enables agents to learn a concept via local information exchange, and to continuously adapt to track possible concept drifts. Distributed implementations offer an attractive alternative to centralized solutions with advantages related to scalability, robustness, and decentralization (see, e.g., [2], [3] and the many examples therein). Several strategies for distributed online parameter estimation have been proposed in the literature, including consensus strategies [4]–[9], incremental strategies [10]–[14], and diffusion strategies [15]–[20]. Incremental techniques operate on a cyclic path that runs across all nodes, which makes them sensitive to link failures and problematic for adaptive implementations. On the other hand, diffusion strategies are particularly attractive due to their enhanced adaptation performance and wider stability ranges than consensus-based implementations. Accessible overviews of results on diffusion adaptation can be found in [2], [15], [16].

Most prior literature focuses primarily on the case where nodes estimate a single parameter vector collaboratively. We refer to problems of this type as single-task problems. Some applications require more complex models and flexible algorithms than single-task implementations since their agents may involve the need to track multiple targets simultaneously. For instance, sensor networks deployed to estimate a spatially-varying temperature profile need to exploit more directly the spatio-temporal correlations that exist between measurements at neighboring nodes [21]. Likewise, monitoring applications where agents need to track the movement of multiple correlated targets need to exploit the correlation profile in the data for enhanced accuracy. Problems of this kind, where nodes need to infer multiple parameter vectors, are referred to as multitask problems.

Existing strategies to address multitask problems mostly depend on how the tasks relate to each other and on exploiting some prior information. There have been a couple of useful works dealing with such problems over distributed networks. For example, in [22], a diffusion strategy is used to solve a distributed estimation problem with nodes that simultaneously estimate local and global parameters. In comparison, the parameter space is decomposed into two orthogonal subspaces in [23], with one of the subspaces being common to all nodes. A multitask estimation algorithm over a fully connected broadcasting network is also considered in [24], [25]. These works assume that the node-specific parameter vectors lie in a common latent signal subspace and exploit this property to compress information and to reduce communication costs. An alternative way to exploit and model relationships among tasks is to formulate optimization problems with appropriate co-regularizers between nodes. The multitask diffusion LMS algorithm derived in [26] relies on this principle, and we build on this construction in this article. In this context, the network is not assumed to be fully connected and agents need not be interested in some common parameters. It is sufficient to assume that different clusters within the network are interested in their own models, and that there are some correlation among the models of adjacent clusters. This correlation is captured by means of regularization parameters.

The aforementioned works on multitask problems assume that all agents respond to data synchronously. In several applications, agents may not be able to act synchronously because networks can be subject to several sources of

uncertainties such as changing topology, random link failures, or agents turning on and off. There exist several useful studies in the literature on the performance of consensus and gossip strategies in the presence of asynchronous events [8], [9], [27], [28] or changing topologies [8], [9], [28]–[34]. In most parts, these works investigate pure averaging algorithms that cannot process streaming data or the works assume noise-free data or make use of decreasing step-size sequences. There are also studies in the context of diffusion strategies. In particular, the works [35]–[37] advanced a rather general framework for asynchronous networks that includes many prior models as special cases. The works examined how asynchronous events interfere with the behavior of adaptive networks in the presence of streaming noisy data and under constant step-size adaptation. Several interesting conclusions are reported in [37] where comparisons are carried out between synchronous and asynchronous behavior, as well as with centralized solutions. In the current work, we would like to examine similar effects to [35], [36] albeit in the context of multitask networks as opposed to single-task networks. In this case, a new dimension arises in that asynchronous events can interfere with the exchange of information among clusters. We examine in some detail the mean and mean-square stability of the multitask network and show that sufficiently step-sizes can still ensure convergence and performance. Various simulation results illustrate the theoretical findings.

This paper is organized as follows. In Section II, we briefly recall the multitask diffusion LMS strategy and we introduce a fairly general model for asynchronous behavior. Under this model, agents in the network may stop updating their solutions, or may stop sending or receiving information in a random manner. Section III analyzes the theoretical performance of the algorithm, in the mean and mean-square error sense. In Section IV, experiments are presented to illustrate the performance of the diffusion multitask approach over asynchronous networks.

II. MULTITASK DIFFUSION LMS OVER ASYNCHRONOUS NETWORKS

Before starting our presentation, we provide a summary of some of the main symbols used in the article. Other symbols will be defined in the context where they are used:

- x Normal font letters denote scalars.
- \mathbf{x} Boldface lowercase letters denote column vectors.
- \mathbf{R} Boldface uppercase letters denote matrices.
- $(\cdot)^\top$ Matrix transpose.
- $(\cdot)^{-1}$ Matrix inverse.
- \mathbf{I}_N Identity matrix of size $N \times N$.
- \mathcal{N}_k The set of nodes containing the neighborhood of node k , including k .
- \mathcal{N}_k^- The set of nodes containing the neighborhood of node k , excluding k .
- \mathcal{C}_j Cluster j , i.e., index set of nodes in the j -th cluster.
- $\mathcal{C}(k)$ The cluster of nodes to which node k belongs, including k .
- $\mathcal{C}(k)^-$ The cluster of nodes to which node k belongs, excluding k .

We now briefly recall the *synchronous* diffusion adaptation strategy developed in [26] for solving distributed optimization problems over multitask networks.

A. Multitask diffusion adaptation

We consider a connected network consisting of N nodes grouped into Q clusters, as illustrated in Figure 1. The problem is to estimate an $L \times 1$ unknown vector \mathbf{w}_k^* at each node k from collected data. Node k has access to temporal measurement sequences $\{d_k(i), \mathbf{x}_k(i)\}$, where $d_k(i)$ is a scalar zero-mean reference signal, and $\mathbf{x}_k(i)$ is an $L \times 1$ regression vector with a positive-definite covariance matrix $\mathbf{R}_{x,k} = E\{\mathbf{x}_k(i)\mathbf{x}_k^\top(i)\} > 0$. The data at node k are assumed to be related via the linear regression model

$$d_k(i) = \mathbf{x}_k^\top(i) \mathbf{w}_k^* + z_k(i), \quad (1)$$

where $z_k(i)$ is a zero-mean i.i.d. noise of variance $\sigma_{z,k}^2$ that is independent of any other signal. We assume that nodes belonging to the same cluster have the same parameter vector to estimate, namely,

$$\mathbf{w}_k^* = \mathbf{w}_{\mathcal{C}_q}^*, \quad \text{whenever } k \in \mathcal{C}_q. \quad (2)$$

We say that two clusters are connected if there exists at least one edge linking a node from one cluster to a node in the other cluster. We also assume that relationships between connected clusters exist so that cooperation among adjacent clusters is beneficial. In particular, we suppose that the parameter vectors corresponding to two connected clusters \mathcal{C}_p and \mathcal{C}_q satisfy certain properties, such as being close to each other [26]. Cooperation across these clusters can therefore be beneficial to infer $\mathbf{w}_{\mathcal{C}_p}^*$ and $\mathbf{w}_{\mathcal{C}_q}^*$.

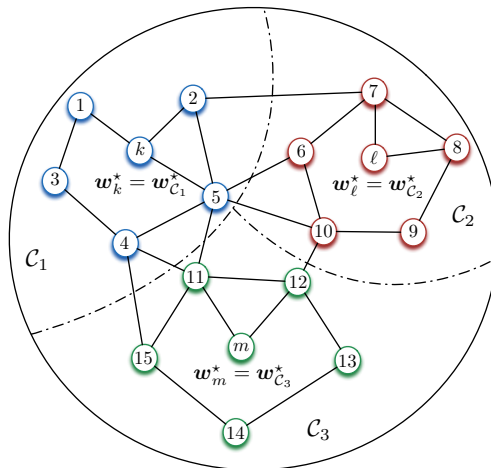


Fig. 1. Clustered network consisting of 3 clusters. Two clusters are connected if they share at least one edge.

Consider the cluster $\mathcal{C}(k)$ to which node k belongs. A local cost function, $J_k(\mathbf{w}_{\mathcal{C}(k)})$, is associated with node k . It is assumed to be strongly convex and second-order differentiable, an example of which is the mean-square error criterion considered throughout this paper and defined by

$$J_k(\mathbf{w}_{\mathcal{C}(k)}) = \mathbb{E}\{|d_k(i) - \mathbf{x}_k^\top(i) \mathbf{w}_{\mathcal{C}(k)}|^2\}. \quad (3)$$

Depending on the application, there may be certain properties among the optimal vectors $\{\mathbf{w}_{\mathcal{C}_1}^*, \dots, \mathbf{w}_{\mathcal{C}_Q}^*\}$ that deserve to be promoted in order to enhance estimation accuracy. Among other possible options, a smoothness condition was enforced in [26]. Specifically, the local variation of the graph signal at node k was defined as the squared ℓ_2 -norm of the graph gradient at this node [38], namely,

$$\|\nabla_k \mathcal{W}\|^2 = \sum_{\ell \in \mathcal{N}_k} \rho_{k\ell} \|\mathbf{w}_k - \mathbf{w}_\ell\|^2 \quad (4)$$

where $\rho_{k\ell}$ is a nonnegative weight assigned to the edge between nodes k and ℓ . As an alternative to (4), it was also proposed in [26] to use the ℓ_1 -norm of the graph gradient at each node in order to promote piecewise constant transitions in the entries of the parameter vectors. In this paper, we will focus on (4).

To estimate the unknown parameter vectors $\mathbf{w}_{\mathcal{C}_1}^*, \dots, \mathbf{w}_{\mathcal{C}_Q}^*$, it was shown in [26] that the local cost (3) and the regularizer (4) can be combined at the level of each cluster. This formulation led to the following estimation problem defined in terms of Q Nash equilibrium problems [39], where each cluster \mathcal{C}_j estimates $\mathbf{w}_{\mathcal{C}_j}^*$ by minimizing the regularized cost function $J_{\mathcal{C}_j}(\mathbf{w}_{\mathcal{C}_j}, \mathbf{w}_{-\mathcal{C}_j})$:

$$(\mathcal{P}_j) \begin{cases} \min_{\mathbf{w}_{\mathcal{C}_j}} J_{\mathcal{C}_j}(\mathbf{w}_{\mathcal{C}_j}, \mathbf{w}_{-\mathcal{C}_j}) \\ \text{with } J_{\mathcal{C}_j}(\mathbf{w}_{\mathcal{C}_j}, \mathbf{w}_{-\mathcal{C}_j}) = \sum_{k \in \mathcal{C}_j} \mathbb{E}\{|d_k(i) - \mathbf{x}_k^\top(i) \mathbf{w}_{\mathcal{C}(k)}|^2\} + \eta \sum_{k \in \mathcal{C}_j} \sum_{\ell \in \mathcal{N}_k \setminus \mathcal{C}_j} \rho_{k\ell} \|\mathbf{w}_{\mathcal{C}(k)} - \mathbf{w}_{\mathcal{C}(\ell)}\|^2 \end{cases} \quad (5)$$

for $j = 1, \dots, Q$. Note that we have kept the notation $\mathbf{w}_{\mathcal{C}(k)}$ in (5) to make the role of the regularization term clearer, even though we have $\mathbf{w}_{\mathcal{C}(k)} = \mathbf{w}_{\mathcal{C}_j}$ for all k in \mathcal{C}_j . The notation $\mathbf{w}_{-\mathcal{C}_j}$ denotes the collection of weight vectors estimated by the other clusters, that is, $\mathbf{w}_{-\mathcal{C}_j} = \{\mathbf{w}_{\mathcal{C}_q} : q = 1, \dots, Q\} - \{\mathbf{w}_{\mathcal{C}_j}\}$. The second term on the RHS of expression (5) enforces smoothness of the resulting graph parameter vectors $\{\mathbf{w}_{\mathcal{C}_1}, \dots, \mathbf{w}_{\mathcal{C}_Q}\}$, with strength parameter $\eta \geq 0$. In [26], the coefficients $\{\rho_{k\ell}\}$ were chosen to satisfy the conditions:

$$\sum_{\ell \in \mathcal{N}_k \setminus \mathcal{C}(k)^-} \rho_{k\ell} = 1, \text{ and } \begin{cases} \rho_{k\ell} > 0, \text{ if } \ell \in \mathcal{N}_k \setminus \mathcal{C}(k), \\ \rho_{kk} \geq 0, \\ \rho_{k\ell} = 0, \text{ otherwise.} \end{cases} \quad (6)$$

We impose $\rho_{k\ell} = 0$ for all $\ell \notin \mathcal{N}_k \setminus \mathcal{C}(k)$ since nodes belonging to the same cluster estimate the same parameter vector.

Following the same line of reasoning from [16], [18] in the single-task case, and extending the argument to problem (5) by using Nash-equilibrium properties [39], [40], the following diffusion strategy of the adapt-then-combine (ATC) form was derived in [26] for solving the multitask learning problem (5) in a distributed manner:

$$\begin{cases} \boldsymbol{\psi}_k(i+1) = \mathbf{w}_k(i) + \mu_k \mathbf{x}_k(i) (d_k(i) - \mathbf{x}_k^\top(i) \mathbf{w}_k(i)) + \eta \mu_k \left(\sum_{\ell \in \mathcal{N}_k \setminus \mathcal{C}(k)^-} \rho_{k\ell} (\mathbf{w}_\ell(i) - \mathbf{w}_k(i)) \right), \\ \mathbf{w}_k(i+1) = \sum_{\ell \in \mathcal{N}_k \cap \mathcal{C}(k)} a_{\ell k} \boldsymbol{\psi}_\ell(i+1). \end{cases} \quad (7)$$

where $\mathbf{w}_k(i)$ denotes the estimate of the unknown parameter vector \mathbf{w}_k^* at node k and iteration i , and μ_k is a positive step-size parameter. The combination coefficients $\{a_{\ell k}\}$ are nonnegative scalars that are chosen to satisfy

the conditions:

$$\sum_{\ell \in \mathcal{N}_k \cap \mathcal{C}(k)} a_{\ell k} = 1, \text{ and } \begin{cases} a_{\ell k} > 0, & \text{if } \ell \in \mathcal{N}_k \cap \mathcal{C}(k), \\ a_{\ell k} = 0, & \text{otherwise.} \end{cases} \quad (8)$$

There are several ways to select these coefficients such as using the averaging rule or the Metropolis rule (see [16] for a listing of these and other choices).

B. Asynchronous multitask diffusion adaptation

To model the asynchronous behavior over networks, we follow the same procedure developed in [35] since the model presented in that work allows us to cover many situations of practical interest. Specifically, we replace each deterministic step-size μ_k by a random process $\mu_k(i)$, and model uncertainties in the links by using *random* combination coefficients $\{a_{\ell k}(i)\}$ and *random* regularization factors $\{\rho_{k\ell}(i)\}$. In other words, we modify the multitask diffusion strategy (7) to the following form:

$$\begin{cases} \boldsymbol{\psi}_k(i+1) = \mathbf{w}_k(i) + \mu_k(i) \mathbf{x}_k(i) (d_k(i) - \mathbf{x}_k^\top(i) \mathbf{w}_k(i)) + \eta \mu_k(i) \left(\sum_{\ell \in \mathcal{N}_k(i) \setminus \mathcal{C}(k)} \rho_{k\ell}(i) (\mathbf{w}_\ell(i) - \mathbf{w}_k(i)) \right), \\ \mathbf{w}_k(i+1) = \sum_{\ell \in \mathcal{N}_k(i) \cap \mathcal{C}(k)} a_{\ell k}(i) \boldsymbol{\psi}_\ell(i+1) \end{cases} \quad (9)$$

where $\mathcal{N}_k(i)$ is also now random and denotes the random neighborhood of agent k at time instant i . The composition of each cluster is assumed to be known a-priori and does not change over time. In a manner similar to [35], the asynchronous network model is assumed to satisfy the following conditions:

- *Conditions on the step-size parameters:* At each time instant i , the step-size at node k is a bounded non-negative random variable $\mu_k(i) \in [0, \mu_{\max, k}]$. These step-sizes are collected into the random matrix $\mathbf{M}(i) \triangleq \text{diag}\{\mu_1(i), \dots, \mu_N(i)\}$. We assume that $\{\mathbf{M}(i), i \geq 0\}$ is a weakly stationary random process with mean $\overline{\mathbf{M}}$ and Kronecker-covariance matrix \mathbf{C}_M of size $N^2 \times N^2$ defined as

$$\mathbf{C}_M \triangleq \mathbb{E}\{(\mathbf{M}(i) - \overline{\mathbf{M}}) \otimes (\mathbf{M}(i) - \overline{\mathbf{M}})\} \quad (10)$$

with \otimes denoting the Kronecker product.

- *Conditions on the combination coefficients:* The random coefficients $\{a_{\ell k}(i)\}$ used to scale the estimates $\{\boldsymbol{\psi}_\ell(i+1)\}$ that are being received by node k from its cluster neighbors $\ell \in \mathcal{N}_k(i) \cap \mathcal{C}(k)$ satisfy the following constraints at each iteration i :

$$\sum_{\ell \in \mathcal{N}_k(i) \cap \mathcal{C}(k)} a_{\ell k}(i) = 1, \text{ and } \begin{cases} a_{\ell k}(i) > 0, & \text{if } \ell \in \mathcal{N}_k(i) \cap \mathcal{C}(k), \\ a_{\ell k}(i) = 0, & \text{otherwise.} \end{cases} \quad (11)$$

We collect these coefficients into the random $N \times N$ left-stochastic matrix $\mathbf{A}(i)$. We again assume that $\{\mathbf{A}(i), i \geq 0\}$ is a weakly stationary random process. Let $\overline{\mathbf{A}}$ be its mean and \mathbf{C}_A its Kronecker-covariance matrix of size $N^2 \times N^2$ defined as

$$\mathbf{C}_A \triangleq \mathbb{E}\{(\mathbf{A}(i) - \overline{\mathbf{A}}) \otimes (\mathbf{A}(i) - \overline{\mathbf{A}})\}. \quad (12)$$

- *Conditions on the regularization factors:* The random factors $\{\rho_{k\ell}(i)\}$, which adjust the regularization strength between the parameter vectors at neighboring nodes of distinct clusters, satisfy the following constraints at each iteration i :

$$\sum_{\ell \in \mathcal{N}_k(i) \setminus \mathcal{C}(k)^-} \rho_{k\ell}(i) = 1, \text{ and } \begin{cases} \rho_{k\ell}(i) > 0, & \text{if } \ell \in \mathcal{N}_k(i) \setminus \mathcal{C}(k), \\ \rho_{kk}(i) \geq 0, \\ \rho_{k\ell}(i) = 0, & \text{otherwise.} \end{cases} \quad (13)$$

We collect these coefficients into the random $N \times N$ right-stochastic matrix $\mathbf{P}(i)$. We assume that $\{\mathbf{P}(i), i \geq 0\}$ is a weakly stationary random process with mean $\bar{\mathbf{P}}$ and Kronecker-covariance matrix \mathbf{C}_P of size $N^2 \times N^2$ defined as

$$\mathbf{C}_P \triangleq \mathbb{E}\{(\mathbf{P}(i) - \bar{\mathbf{P}}) \otimes (\mathbf{P}(i) - \bar{\mathbf{P}})\}. \quad (14)$$

- *Independence assumptions:* The random matrices $\mathbf{M}(i)$, $\mathbf{A}(i)$ and $\mathbf{P}(i)$ at iteration i are mutually-independent, and independent of any other random variables.
- *Mean graph:* The mean matrices $\bar{\mathbf{A}}$ and $\bar{\mathbf{P}}$ define the intra-cluster and inter-cluster neighborhoods, namely, $\mathcal{N}_k \cap \mathcal{C}(k)$ and $\mathcal{N}_k \setminus \mathcal{C}(k)$ for all k , respectively. We refer to the neighborhoods $\{\mathcal{N}_k\}$ defined by $\bar{\mathbf{A}}$ and $\bar{\mathbf{P}}$ as the mean graph. In view of the above conditions, the mean combination coefficients $\bar{a}_{\ell k} \triangleq \mathbb{E}\{a_{\ell k}(i)\}$ and regularization factors $\bar{\rho}_{k\ell} \triangleq \mathbb{E}\{\rho_{k\ell}(i)\}$ are nonnegative and satisfy the following constraints.

$$\sum_{\ell \in \mathcal{N}_k \cap \mathcal{C}(k)} \bar{a}_{\ell k} = 1, \text{ and } \begin{cases} \bar{a}_{\ell k} > 0, & \text{if } \ell \in \mathcal{N}_k \cap \mathcal{C}(k), \\ \bar{a}_{\ell k} = 0, & \text{otherwise,} \end{cases} \quad (15)$$

$$\sum_{\ell \in \mathcal{N}_k \setminus \mathcal{C}(k)^-} \bar{\rho}_{k\ell} = 1, \text{ and } \begin{cases} \bar{\rho}_{k\ell} > 0, & \text{if } \ell \in \mathcal{N}_k \setminus \mathcal{C}(k), \\ \bar{\rho}_{kk} \geq 0, \\ \bar{\rho}_{k\ell} = 0, & \text{otherwise.} \end{cases} \quad (16)$$

Using the same arguments as Lemmas 2 and 3 in [35], we can state the following properties for the asynchronous model (9).

Property 1. *The $N \times N$ matrix $\bar{\mathbf{A}}$ and the $N^2 \times N^2$ matrix $\bar{\mathbf{A}} \otimes \bar{\mathbf{A}} + \mathbf{C}_A$ are left-stochastic matrices.*

Property 2. *The $N \times N$ matrix $\bar{\mathbf{P}}$ and the $N^2 \times N^2$ matrix $\bar{\mathbf{P}} \otimes \bar{\mathbf{P}} + \mathbf{C}_P$ are right-stochastic matrices.*

Property 3. *For every node k , the neighborhood \mathcal{N}_k that is defined by the mean graph of the asynchronous model (9) is equal to the union of all possible realizations for the random neighborhood $\mathcal{N}_k(i)$, that is,*

$$\mathcal{N}_k = \bigcup_{\omega \in \Omega} \mathcal{N}_k(\omega) \quad (17)$$

where Ω denotes the sample space of the random neighborhoods $\mathcal{N}_k(i)$.

We provide in Appendix A one example for a common asynchronous network referred to as the Bernoulli network.

III. PERFORMANCE OF MULTITASK DIFFUSION OVER ASYNCHRONOUS NETWORKS

The performance of the multitask diffusion algorithm (9) is affected by the various random perturbations due to the asynchronous events. We now examine the stochastic behavior of this strategy in the mean and mean-square error sense.

A. Mean error behavior analysis

For each agent k , we introduce the weight error vectors:

$$\tilde{\mathbf{w}}_k(i) \triangleq \mathbf{w}_k^* - \mathbf{w}_k(i), \quad \tilde{\boldsymbol{\psi}}_k(i) \triangleq \mathbf{w}_k^* - \boldsymbol{\psi}_k(i) \quad (18)$$

where \mathbf{w}_k^* is the optimum parameter vector at node k . We denote by $\tilde{\mathbf{w}}(i)$, $\tilde{\boldsymbol{\psi}}(i)$ and \mathbf{w}^* the block weight error vector, the block intermediate weight error vector, and the block optimum weight vector, all of size $N \times 1$ with blocks of size $L \times 1$, namely,

$$\tilde{\mathbf{w}}(i) \triangleq \text{col}\{\tilde{\mathbf{w}}_1(i), \dots, \tilde{\mathbf{w}}_N(i)\} \quad (19)$$

$$\tilde{\boldsymbol{\psi}}(i) \triangleq \text{col}\{\tilde{\boldsymbol{\psi}}_1(i), \dots, \tilde{\boldsymbol{\psi}}_N(i)\} \quad (20)$$

$$\mathbf{w}^* \triangleq \text{col}\{\mathbf{w}_1^*, \dots, \mathbf{w}_N^*\}. \quad (21)$$

We also introduce the following $N \times N$ block matrices with individual entries of size $L \times L$:

$$\mathcal{M}(i) \triangleq \mathbf{M}(i) \otimes \mathbf{I}_L \quad (22)$$

$$\mathcal{A}(i) \triangleq \mathbf{A}(i) \otimes \mathbf{I}_L \quad (23)$$

$$\mathcal{P}(i) \triangleq \mathbf{P}(i) \otimes \mathbf{I}_L. \quad (24)$$

To perform the theoretical analysis, we introduce the following independence assumption.

Assumption 1. (*Independent regressors*) *The regression vectors $\mathbf{x}_k(i)$ arise from a stationary random process that is temporally stationary, temporally white, and independent over space with $\mathbf{R}_{x,k} = E\{\mathbf{x}_k(i) \mathbf{x}_k^\top(i)\} > 0$.*

A direct consequence is that $\mathbf{x}_k(i)$ is independent of $\tilde{\mathbf{w}}_\ell(j)$ for all ℓ and $j \leq i$. Although not true in general, this assumption is commonly used to analyze adaptive constructions since it allows to simplify the derivations without constraining the conclusions. There are several results in the adaptation literature that show that performance results that are obtained under the above independence assumptions match well the actual performance of the algorithms when the step-sizes are sufficiently small (see, e.g., [41, App. 24.A] and the many references therein).

The estimation error in the first step of the asynchronous strategy (9) can be rewritten as:

$$d_k(i) - \mathbf{x}_k^\top(i) \mathbf{w}_k(i) = \mathbf{x}_k^\top(i) \tilde{\mathbf{w}}_k(i) + z_k(i). \quad (25)$$

Subtracting \mathbf{w}_k^* from both sides of the adaptation step in (9) and using the above relation, we can express the update equation for $\tilde{\boldsymbol{\psi}}(i+1)$ as:

$$\tilde{\boldsymbol{\psi}}(i+1) = [\mathbf{I}_{NL} - \mathcal{M}(i)(\mathcal{R}_x(i) + \eta \mathcal{Q}(i))] \tilde{\mathbf{w}}(i) - \mathcal{M}(i) \mathbf{p}_{xz}(i) + \eta \mathcal{M}(i) \mathcal{Q}(i) \mathbf{w}^* \quad (26)$$

where

$$\mathcal{Q}(i) \triangleq \mathbf{I}_{NL} - \mathcal{P}(i), \quad (27)$$

while $\mathcal{R}_x(i)$ is an $N \times N$ block matrix with individual entries of size $L \times L$ given by

$$\mathcal{R}_x(i) \triangleq \text{diag}\{\mathbf{x}_1(i)\mathbf{x}_1^\top(i), \dots, \mathbf{x}_N(i)\mathbf{x}_N^\top(i)\}, \quad (28)$$

and $\mathbf{p}_{xz}(i)$ is the $N \times 1$ block column vector with blocks of size $L \times 1$ defined as

$$\mathbf{p}_{xz}(i) \triangleq \text{col}\{\mathbf{x}_1(i)z_1(i), \dots, \mathbf{x}_N(i)z_N(i)\}. \quad (29)$$

Subtracting \mathbf{w}_k^* from both sides of the combination step in (9), we get the block weight error vector:

$$\tilde{\mathbf{w}}(i+1) = \mathcal{A}^\top(i) \tilde{\boldsymbol{\psi}}(i+1). \quad (30)$$

Substituting (26) into (30) we find that the error dynamics of the asynchronous multitask diffusion strategy (9) evolves according to the following recursion:

$$\tilde{\mathbf{w}}(i+1) = \mathcal{A}^\top(i) [\mathbf{I}_{NL} - \mathcal{M}(i)(\mathcal{R}_x(i) + \eta \mathcal{Q}(i))] \tilde{\mathbf{w}}(i) - \mathcal{A}^\top(i) \mathcal{M}(i) \mathbf{p}_{xz}(i) + \eta \mathcal{A}^\top(i) \mathcal{M}(i) \mathcal{Q}(i) \mathbf{w}^*. \quad (31)$$

For compactness of notation, we introduce the symbols:

$$\mathcal{B}(i) \triangleq \mathcal{A}^\top(i) [\mathbf{I}_{NL} - \mathcal{M}(i)(\mathcal{R}_x(i) + \eta \mathcal{Q}(i))] \quad (32)$$

$$\mathbf{g}(i) \triangleq \mathcal{A}^\top(i) \mathcal{M}(i) \mathbf{p}_{xz}(i) \quad (33)$$

$$\mathbf{r}(i) \triangleq \mathcal{A}^\top(i) \mathcal{M}(i) \mathcal{Q}(i) \mathbf{w}^*, \quad (34)$$

so that (31) can be written as

$$\tilde{\mathbf{w}}(i+1) = \mathcal{B}(i) \tilde{\mathbf{w}}(i) - \mathbf{g}(i) + \eta \mathbf{r}(i). \quad (35)$$

Taking the expectation of both sides, using Assumption 1 and the independence of $\mathcal{A}(i)$, $\mathcal{M}(i)$ and $\mathcal{P}(i)$, the network mean error vector ends up evolving according to the following dynamics:

$$\mathbb{E}\{\tilde{\mathbf{w}}(i+1)\} = \mathcal{B} \mathbb{E}\{\tilde{\mathbf{w}}(i)\} + \eta \mathbf{r} \quad (36)$$

where

$$\mathcal{B} \triangleq \mathbb{E}\{\mathcal{B}(i)\} = \mathcal{A}^\top [\mathbf{I}_{NL} - \mathcal{M}(\mathcal{R}_x + \eta \mathcal{Q})] \quad (37)$$

$$\mathbf{r} \triangleq \mathbb{E}\{\mathbf{r}(i)\} = \mathcal{A}^\top \mathcal{M} \mathcal{Q} \mathbf{w}^*, \quad (38)$$

where \mathcal{A} , \mathcal{M} , \mathcal{R}_x and \mathcal{Q} denote the expectations of $\mathcal{A}(i)$, $\mathcal{M}(i)$, $\mathcal{R}_x(i)$ and $\mathcal{Q}(i)$, respectively, and are given by:

$$\mathcal{A} \triangleq \mathbb{E}\{\mathcal{A}(i)\} = \bar{\mathbf{A}} \otimes \mathbf{I}_L \quad (39)$$

$$\mathcal{M} \triangleq \mathbb{E}\{\mathcal{M}(i)\} = \bar{\mathbf{M}} \otimes \mathbf{I}_L \quad (40)$$

$$\mathcal{P} \triangleq \mathbb{E}\{\mathcal{P}(i)\} = \bar{\mathbf{P}} \otimes \mathbf{I}_L \quad (41)$$

$$\mathcal{R}_x \triangleq \mathbb{E}\{\mathcal{R}_x(i)\} = \text{diag}\{\mathbf{R}_{x,1}, \dots, \mathbf{R}_{x,N}\} \quad (42)$$

$$\mathcal{Q} \triangleq \mathbb{E}\{\mathcal{Q}(i)\} = \mathbf{I}_{NL} - \mathbb{E}\{\mathcal{P}(i)\} = \mathbf{I}_{NL} - \mathcal{P}. \quad (43)$$

Note that $\mathbb{E}\{\mathbf{g}(i)\} = \mathbf{0}$ since $z_k(i)$ is zero-mean and independent of any other signal.

Theorem 1. (Stability in the mean) Assume data model (1) and Assumption 1 hold. Then, for any initial condition, the multitask diffusion LMS strategy (9) applied to asynchronous networks converges asymptotically in the mean if, and only if, the step-sizes in \mathcal{M} are chosen to satisfy

$$\rho(\mathcal{A}^\top [\mathbf{I}_{NL} - \mathcal{M}(\mathcal{R}_x + \eta\mathcal{Q})]) < 1, \quad (44)$$

where $\rho(\cdot)$ denotes the spectral radius of its matrix argument. In that case, the asymptotic mean bias is given by

$$\lim_{i \rightarrow \infty} \mathbb{E}\{\tilde{\mathbf{w}}(i)\} = \eta (\mathbf{I}_{NL} - \mathcal{B})^{-1} \mathbf{r}. \quad (45)$$

Assume that the expected values for all step-sizes are uniform, namely, $\mathbb{E}\{\mu_k(i)\} = \bar{\mu}$ for all k . A sufficient condition for (44) to hold is to ensure that

$$0 < \bar{\mu} < \frac{2}{\max_{1 \leq k \leq N} \rho(\mathcal{R}_{x,k}) + 2\eta}. \quad (46)$$

Proof: Convergence in the mean requires the matrix \mathcal{B} in (36) to be stable. Since any induced matrix norm is lower bounded by its spectral radius, we can write in terms of the block maximum norm [16]:

$$\begin{aligned} \rho(\mathcal{A}^\top [\mathbf{I}_{NL} - \mathcal{M}(\mathcal{R}_x + \eta\mathcal{Q})]) &\leq \|\mathcal{A}^\top [\mathbf{I}_{NL} - \mathcal{M}(\mathcal{R}_x + \eta\mathcal{Q})]\|_{b,\infty} \\ &\leq \|\mathcal{A}^\top\|_{b,\infty} \cdot \|\mathbf{I}_{NL} - \mathcal{M}(\mathcal{R}_x + \eta\mathcal{Q})\|_{b,\infty}. \end{aligned} \quad (47)$$

We have $\|\mathcal{A}^\top\|_{b,\infty} = 1$ because \mathcal{A} is a block left-stochastic matrix. This yields:

$$\begin{aligned} \rho(\mathcal{A}^\top [\mathbf{I}_{NL} - \mathcal{M}(\mathcal{R}_x + \eta\mathcal{Q})]) &\leq \|\mathbf{I}_{NL} - \mathcal{M}(\mathcal{R}_x + \eta\mathcal{Q})\|_{b,\infty} \\ &= \|\mathbf{I}_{NL} - \mathcal{M}(\mathcal{R}_x + \eta(\mathbf{I}_{NL} - \mathcal{P}))\|_{b,\infty} \\ &\leq \|\mathbf{I}_{NL} - \mathcal{M}\mathcal{R}_x - \eta\mathcal{M}\|_{b,\infty} + \eta\|\mathcal{M}\mathcal{P}\|_{b,\infty}. \end{aligned} \quad (48)$$

Consider the first term on the RHS of (48). Since the matrices \mathcal{M} , \mathcal{R}_x are block diagonal, it holds from the properties of the block maximum norm [16]:

$$\begin{aligned} \|\mathbf{I}_{NL} - \mathcal{M}\mathcal{R}_x - \eta\mathcal{M}\|_{b,\infty} &= \max_{1 \leq k \leq N} \rho((1 - \eta\bar{\mu}_k)\mathbf{I}_L - \bar{\mu}_k\mathcal{R}_{x,k}) \\ &= \max_{1 \leq k \leq N} \max_{1 \leq \ell \leq L} |(1 - \eta\bar{\mu}_k) - \bar{\mu}_k\lambda_\ell(\mathcal{R}_{x,k})| \end{aligned} \quad (49)$$

where $\bar{\mu}_k \triangleq \mathbb{E}\{\mu_k(i)\}$, and $\lambda_\ell(\cdot)$ denotes the ℓ -th eigenvalue of its matrix argument. Consider now the second term on the RHS of (48). Using the submultiplicative property of the block maximum norm, and the fact that \mathcal{P} is a block right-stochastic matrix, we get

$$\eta\|\mathcal{M}\mathcal{P}\|_{b,\infty} \leq \eta\|\mathcal{M}\|_{b,\infty}. \quad (50)$$

Because \mathcal{M} is a block diagonal matrix, we further have that

$$\|\mathcal{M}\|_{b,\infty} = \max_{1 \leq k \leq N} \bar{\mu}_k. \quad (51)$$

Combining (49) and (51) we conclude that the algorithm is stable in the mean if

$$\max_{1 \leq k \leq N} \max_{1 \leq \ell \leq L} |1 - \eta \bar{\mu}_k - \bar{\mu}_k \lambda_\ell(\mathbf{R}_{x,k})| + \eta \max_{1 \leq k \leq N} \bar{\mu}_k < 1. \quad (52)$$

In order to simplify this condition, assume that $\bar{\mu}_k = \mu$ for all k . Condition (52) then reduces to (46). Note that the randomness in the topology does not affect the condition for stability in the mean of the algorithm. ■

B. Mean-square error behavior analysis

To perform the mean-square error analysis, we shall use the block Kronecker product operator \otimes_b instead of the Kronecker product \otimes , and the block vectorization operator $\text{bvec}(\cdot)$ instead of the vectorization operator $\text{vec}(\cdot)$. This is because, as explained in [3], [36], these block operators preserve the locality of the blocks in the original matrix arguments. Recall that if \mathbf{X} is an $N \times N$ block matrix with blocks of size $L \times L$, $\text{bvec}(\mathbf{X})$ vectorizes each block of \mathbf{X} and stacks the vectors on top of each other. Before proceeding, we recall some properties of these block operators [3], [42]:

For any two $N \times 1$ block vectors $\{\mathbf{x}, \mathbf{y}\}$ with blocks of size $L \times 1$, we have:

$$\text{bvec}(\mathbf{x}\mathbf{y}^\top) = \mathbf{y} \otimes_b \mathbf{x}. \quad (53)$$

For any $N \times N$ block-matrices $\{\mathbf{A}, \mathbf{B}, \mathbf{C}, \mathbf{D}\}$ with blocks of size $L \times L$, we have:

$$(\mathbf{A} + \mathbf{B}) \otimes_b (\mathbf{C} + \mathbf{D}) = \mathbf{A} \otimes_b \mathbf{C} + \mathbf{A} \otimes_b \mathbf{D} + \mathbf{B} \otimes_b \mathbf{C} + \mathbf{B} \otimes_b \mathbf{D} \quad (54)$$

$$(\mathbf{AC}) \otimes_b (\mathbf{BD}) = (\mathbf{A} \otimes_b \mathbf{B})(\mathbf{C} \otimes_b \mathbf{D}) \quad (55)$$

$$(\mathbf{A} \otimes \mathbf{B}) \otimes_b (\mathbf{C} \otimes \mathbf{D}) = (\mathbf{A} \otimes \mathbf{C}) \otimes (\mathbf{B} \otimes \mathbf{D}) \quad (56)$$

$$\text{trace}(\mathbf{AB}) = [\text{bvec}(\mathbf{B}^\top)]^\top \text{bvec}(\mathbf{A}) \quad (57)$$

$$\text{bvec}(\mathbf{ABC}) = (\mathbf{C}^\top \otimes_b \mathbf{A}) \text{bvec}(\mathbf{B}) \quad (58)$$

$$(\mathbf{A} \otimes_b \mathbf{B})^\top = (\mathbf{A}^\top \otimes_b \mathbf{B}^\top). \quad (59)$$

We now use these properties to evaluate the expectation of some block Kronecker matrix products that will be useful in the sequel:

$$\begin{aligned} \mathcal{M}_I &\triangleq \mathbb{E}\{\mathcal{M}(i) \otimes_b \mathcal{M}(i)\} &= \mathbb{E}\{(\mathbf{M}(i) \otimes \mathbf{I}_L) \otimes_b (\mathbf{M}(i) \otimes \mathbf{I}_L)\} \\ &&\stackrel{(57)}{=} \mathbb{E}\{(\mathbf{M}(i) \otimes \mathbf{M}(i)) \otimes (\mathbf{I}_L \otimes \mathbf{I}_L)\} \\ &&\stackrel{(10)}{=} (\overline{\mathbf{M}} \otimes \overline{\mathbf{M}} + \mathbf{C}_M) \otimes \mathbf{I}_{L^2}. \end{aligned} \quad (60)$$

In the same way, we get the following expectations:

$$\mathcal{A}_I \triangleq \mathbb{E}\{\mathcal{A}(i) \otimes_b \mathcal{A}(i)\} = (\overline{\mathbf{A}} \otimes \overline{\mathbf{A}} + \mathbf{C}_A) \otimes \mathbf{I}_{L^2}, \quad (61)$$

$$\mathcal{P}_I \triangleq \mathbb{E}\{\mathcal{P}(i) \otimes_b \mathcal{P}(i)\} = (\bar{\mathbf{P}} \otimes \bar{\mathbf{P}} + \mathbf{C}_P) \otimes \mathbf{I}_{L^2}. \quad (62)$$

Since $\mathcal{Q}(i) = \mathbf{I}_{NL} - \mathcal{P}(i)$, we also obtain:

$$\mathcal{Q}_I \triangleq \mathbb{E}\{\mathcal{Q}(i) \otimes_b \mathcal{Q}(i)\} = (\mathbf{I}_{N^2} - \mathbf{I}_N \otimes \bar{\mathbf{P}} - \bar{\mathbf{P}} \otimes \mathbf{I}_N + \bar{\mathbf{P}} \otimes \bar{\mathbf{P}} + \mathbf{C}_P) \otimes \mathbf{I}_{L^2}. \quad (63)$$

Before concluding these preliminary calculations, let us make some remarks on the stochasticity of matrices considered in the sequel. At each time instant i , the matrix $\mathcal{P}(i) \otimes \mathcal{P}(i)$ has nonnegative entries since $\mathcal{P}(i)$ has nonnegative entries. It follows that $\mathbb{E}\{\mathcal{P}(i) \otimes \mathcal{P}(i)\} = \bar{\mathbf{P}} \otimes \bar{\mathbf{P}} + \mathbf{C}_P$ has also nonnegative entries, and is right-stochastic since

$$(\bar{\mathbf{P}} \otimes \bar{\mathbf{P}} + \mathbf{C}_P)\mathbf{1}_{N^2} = \mathbb{E}\{(\mathcal{P}(i) \otimes \mathcal{P}(i))(\mathbf{1}_N \otimes \mathbf{1}_N)\} = \mathbb{E}\{(\mathcal{P}(i) \mathbf{1}_N) \otimes (\mathcal{P}(i) \mathbf{1}_N)\} = \mathbf{1}_{N^2} \quad (64)$$

In the same token, the matrix $\bar{\mathbf{A}} \otimes \bar{\mathbf{A}} + \mathbf{C}_A$ is left-stochastic.

To analyze the convergence in mean-square-error sense of the multitask diffusion LMS algorithm (9) over asynchronous networks, we consider the mean-square of the weight error vector $\tilde{\mathbf{w}}(i)$ weighted by any positive semi-definite matrix Σ , that is, $\mathbb{E}\{\|\tilde{\mathbf{w}}(i)\|_{\Sigma}^2\}$, where $\|\tilde{\mathbf{w}}(i)\|_{\Sigma}^2 \triangleq \tilde{\mathbf{w}}^{\top}(i) \Sigma \tilde{\mathbf{w}}(i)$. The freedom in selecting Σ will allow us to extract various types of information about the network and the nodes. By Assumption 1 and using (35), we get:

$$\mathbb{E}\{\|\tilde{\mathbf{w}}(i+1)\|_{\Sigma}^2\} = \mathbb{E}\{\|\tilde{\mathbf{w}}(i)\|_{\Sigma'}^2\} + \mathbb{E}\{\|\mathbf{g}(i)\|_{\Sigma}^2\} + \eta^2 \mathbb{E}\{\|\mathbf{r}(i)\|_{\Sigma}^2\} + 2\eta \mathbb{E}\{\mathbf{r}^{\top}(i) \Sigma \mathcal{B}(i) \tilde{\mathbf{w}}(i)\} \quad (65)$$

where $\Sigma' = \mathbb{E}\{\mathcal{B}^{\top}(i) \Sigma \mathcal{B}(i)\}$. Let σ denotes the $(NL)^2 \times 1$ vector representation of Σ that is obtained by the block vectorization operator, namely, $\sigma \triangleq \text{bvec}(\Sigma)$. In the sequel, it will be more convenient to work with σ than with Σ itself. Let $\sigma' \triangleq \text{bvec}(\Sigma')$. Using property (58), we can verify that

$$\sigma' = \mathcal{F}^{\top} \sigma \quad (66)$$

where \mathcal{F} is the $(NL)^2 \times (NL)^2$ matrix given by:

$$\begin{aligned} \mathcal{F} &\triangleq \mathbb{E}\{\mathcal{B}(i) \otimes_b \mathcal{B}(i)\} \\ &\stackrel{(55)}{=} \mathbb{E}\{\mathcal{A}^{\top}(i) \otimes_b \mathcal{A}^{\top}(i)\} \mathbb{E}\{[\mathbf{I}_{NL} - \mathcal{M}(i)(\mathcal{R}_x(i) + \eta \mathcal{Q}(i))] \otimes_b [\mathbf{I}_{NL} - \mathcal{M}(i)(\mathcal{R}_x(i) + \eta \mathcal{Q}(i))]\} \\ &\stackrel{(61),(54)}{=} \mathcal{A}_I^{\top} [\mathbf{I}_{(NL)^2} - \mathbf{I}_{NL} \otimes_b \mathcal{M}(\mathcal{R}_x + \eta \mathcal{Q}) - \mathcal{M}(\mathcal{R}_x + \eta \mathcal{Q}) \otimes_b \mathbf{I}_{NL} + \\ &\quad \mathbb{E}\{\mathcal{M}(i)(\mathcal{R}_x(i) + \eta \mathcal{Q}(i)) \otimes_b \mathcal{M}(i)(\mathcal{R}_x(i) + \eta \mathcal{Q}(i))\}] \end{aligned} \quad (67)$$

where using property (55) and the definition of \mathcal{M}_I in (60), we have

$$\mathbb{E}\{\mathcal{M}(i)(\mathcal{R}_x(i) + \eta \mathcal{Q}(i)) \otimes_b \mathcal{M}(i)(\mathcal{R}_x(i) + \eta \mathcal{Q}(i))\} = \mathcal{M}_I \mathbb{E}\{(\mathcal{R}_x(i) + \eta \mathcal{Q}(i)) \otimes_b (\mathcal{R}_x(i) + \eta \mathcal{Q}(i))\}. \quad (68)$$

The term on the RHS of equation (68) is proportional to $\mathcal{M}_I = \mathbb{E}\{\mathcal{M}(i) \otimes \mathcal{M}(i)\} \otimes \mathbf{I}_{L^2}$, where $\mathbb{E}\{\mathcal{M}(i) \otimes \mathcal{M}(i)\}$ is an $N \times N$ block diagonal matrix whose k -th block is an $N \times N$ diagonal matrix with ℓ -th entry given by $\mathbb{E}\{\mu_k(i) \mu_{\ell}(i)\}$. It is sufficient for the exposition in this work to focus on the case of sufficiently small step-sizes where terms involving higher order moments of the step-sizes can be ignored. Such approximations are common

when analyzing diffusion strategies in the mean-square-error sense (see [16, Section 6.5]). Accordingly, the last term in (67) can be neglected and we continue our discussion by letting

$$\mathcal{F} = \mathcal{A}_I^\top [I_{(NL)^2} - I_{NL} \otimes_b \mathcal{M}(\mathcal{R}_x + \eta \mathcal{Q}) - \mathcal{M}(\mathcal{R}_x + \eta \mathcal{Q}) \otimes_b I_{NL}]. \quad (69)$$

Consider next the second term on the RHS of (65). We can write:

$$\mathbb{E}\{\|g(i)\|_{\Sigma}^2\} = \text{trace}\{\Sigma \mathbb{E}\{g(i) g^\top(i)\}\} \stackrel{(57)}{=} g_b^\top \sigma \quad (70)$$

where $g_b = \text{bvec}(\mathbb{E}\{g(i) g^\top(i)\})$. Using expression (33) and the definitions of \mathcal{M}_I and \mathcal{A}_I in (60) and (61), we have

$$\begin{aligned} g_b &= \text{bvec}(\mathbb{E}\{(\mathcal{A}^\top(i) \mathcal{M}(i) p_{xz}(i) p_{xz}^\top(i) \mathcal{M}(i) \mathcal{A}(i))\}) \\ &\stackrel{(58)}{=} \mathbb{E}\{(\mathcal{A}^\top(i) \otimes_b \mathcal{A}^\top(i)) \text{bvec}(\mathcal{M}(i) p_{xz}(i) p_{xz}^\top(i) \mathcal{M}(i))\} \\ &\stackrel{(58),(59)}{=} \mathcal{A}_I^\top \mathbb{E}\{(\mathcal{M}(i) \otimes_b \mathcal{M}(i)) \text{bvec}(p_{xz}(i) p_{xz}^\top(i))\} \\ &= \mathcal{A}_I^\top \mathcal{M}_I \text{bvec}(\mathcal{S}), \end{aligned} \quad (71)$$

where $\mathcal{S} \triangleq \mathbb{E}\{p_{xz}(i) p_{xz}^\top(i)\} = \text{diag}\{\sigma_{z,k}^2 \mathbf{R}_{x,k}\}_{k=1}^N$. Let us examine now the third term on the RHS of (65):

$$\mathbb{E}\{\|r(i)\|_{\Sigma}^2\} = \text{trace}\{\Sigma \mathbb{E}\{r(i) r^\top(i)\}\} \stackrel{(57)}{=} r_b^\top \sigma \quad (72)$$

where $r_b = \text{bvec}(\mathbb{E}\{r(i) r^\top(i)\})$. Using expression (34), property (58) and the definitions of \mathcal{M}_I , \mathcal{A}_I and \mathcal{Q}_I in (60), (61) and (63), and proceeding as in (71), we obtain the following expression:

$$r_b = \mathcal{A}_I^\top \mathcal{M}_I \mathcal{Q}_I \text{bvec}(w^*(w^*)^\top). \quad (73)$$

Consider now the fourth term $\mathbb{E}\{r^\top(i) \Sigma \mathcal{B}(i) \tilde{w}(i)\}$. We have:

$$\begin{aligned} \mathbb{E}\{r^\top(i) \Sigma \mathcal{B}(i) \tilde{w}(i)\} &= \mathbb{E}\{\text{bvec}(r^\top(i) \Sigma \mathcal{B}(i) \tilde{w}(i))\} \\ &\stackrel{(58)}{=} \mathbb{E}\{(\mathcal{B}(i) \tilde{w}(i))^\top \otimes_b r^\top(i)\} \sigma \\ &\stackrel{(59)}{=} \mathbb{E}\{\mathcal{B}(i) \tilde{w}(i) \otimes_b r(i)\}^\top \sigma \\ &\stackrel{(55)}{=} \mathbb{E}\{\tilde{w}(i) \otimes_b 1\}^\top \mathbb{E}\{\mathcal{B}(i) \otimes_b r(i)\}^\top \sigma \\ &= \mathbb{E}\{\tilde{w}(i)\}^\top \mathbb{E}\{\mathcal{B}(i) \otimes_b r(i)\}^\top \sigma \end{aligned} \quad (74)$$

with

$$\begin{aligned} \mathbb{E}\{\mathcal{B}(i) \otimes_b r(i)\} &= \mathbb{E}\left\{\mathcal{A}^\top(i) [I_{NL} - \mathcal{M}(i)(\mathcal{R}_x(i) + \eta \mathcal{Q}(i))] \otimes_b \mathcal{A}^\top(i) \mathcal{M}(i) \mathcal{Q}(i) w^*\right\} \\ &\stackrel{(55)}{=} \mathcal{A}_I^\top \mathbb{E}\left\{[I_{NL} - \mathcal{M}(i)(\mathcal{R}_x(i) + \eta \mathcal{Q}(i))] \otimes_b \mathcal{M}(i) \mathcal{Q}(i) w^*\right\} \\ &\stackrel{(54)}{=} \mathcal{A}_I^\top \left[(I_{NL} \otimes_b \mathcal{M} \mathcal{Q} w^*) - \mathbb{E}\{\mathcal{M}(i)(\mathcal{R}_x(i) + \eta \mathcal{Q}(i)) \otimes_b \mathcal{M}(i) \mathcal{Q}(i) w^*\} \right], \end{aligned} \quad (75)$$

where

$$\begin{aligned}
\mathbb{E}\{\mathcal{M}(i)(\mathcal{R}_x(i) + \eta \mathcal{Q}(i)) \otimes_b \mathcal{M}(i) \mathcal{Q}(i) \mathbf{w}^*\} &\stackrel{(55)}{=} \mathcal{M}_I \mathbb{E}\{(\mathcal{R}_x(i) + \eta \mathcal{Q}(i)) \otimes_b \mathcal{Q}(i) \mathbf{w}^*\} \\
&\stackrel{(54)}{=} \mathcal{M}_I ((\mathcal{R}_x \otimes_b \mathcal{Q} \mathbf{w}^*) + \eta \mathbb{E}\{\mathcal{Q}(i) \otimes_b \mathcal{Q}(i) \mathbf{w}^*\}) \\
&\stackrel{(55)}{=} \mathcal{M}_I ((\mathcal{R}_x \otimes_b \mathcal{Q} \mathbf{w}^*) + \eta \mathcal{Q}_I(\mathbf{I}_{NL} \otimes_b \mathbf{w}^*)). \tag{76}
\end{aligned}$$

Finally, combining (75) and (76) and introducing the notation \mathbf{K} , we get

$$\mathbf{K} \triangleq \mathbb{E}\{\mathcal{B}(i) \otimes_b \mathbf{r}(i)\} = \mathcal{A}_I^\top [(\mathbf{I}_{NL} \otimes_b \mathcal{M} \mathcal{Q} \mathbf{w}^*) - \mathcal{M}_I((\mathcal{R}_x \otimes_b \mathcal{Q} \mathbf{w}^*) + \eta \mathcal{Q}_I(\mathbf{I}_{NL} \otimes_b \mathbf{w}^*))]. \tag{77}$$

For compactness, we aggregate the last two terms on the RHS of (65) into:

$$f(\boldsymbol{\sigma}, \mathbb{E}\{\tilde{\mathbf{w}}(i)\}) = \eta^2 \mathbf{r}_b^\top \boldsymbol{\sigma} + 2\eta \mathbb{E}\{\tilde{\mathbf{w}}(i)\}^\top \mathbf{K}^\top \boldsymbol{\sigma}. \tag{78}$$

Then, relation (65) can be written as

$$\mathbb{E}\{\|\tilde{\mathbf{w}}(i+1)\|_{\boldsymbol{\sigma}}^2\} = \mathbb{E}\{\|\tilde{\mathbf{w}}(i)\|_{\mathcal{F}^\top \boldsymbol{\sigma}}^2\} + \mathbf{g}_b^\top \boldsymbol{\sigma} + f(\boldsymbol{\sigma}, \mathbb{E}\{\tilde{\mathbf{w}}(i)\}) \tag{79}$$

where we will be using the notation $\|\cdot\|_{\boldsymbol{\Sigma}}$ and $\|\cdot\|_{\boldsymbol{\sigma}}$ interchangeably.

Theorem 2. (Mean-square stability) *Assume data model (1) and Assumption 1 hold. Assume further that the upper bounds on the step-sizes, $\{\mu_{\max,k}\}$, are sufficiently small such that approximation (69) is justified by ignoring higher-order powers of the step-sizes, and (79) can be used as a reasonable representation for the dynamics of the weighted mean-square error. Then, the asynchronous diffusion multitask algorithm (9) is mean-square stable if the matrix \mathcal{F} defined by (69) is stable.*

Proof: Iterating (79) starting from $i = 0$, we find that:

$$\mathbb{E}\{\|\tilde{\mathbf{w}}(i+1)\|_{\boldsymbol{\sigma}}^2\} = \mathbb{E}\{\|\tilde{\mathbf{w}}(0)\|_{(\mathcal{F}^\top)^{i+1} \boldsymbol{\sigma}}^2\} + \mathbf{g}_b^\top \sum_{j=0}^i (\mathcal{F}^\top)^j \boldsymbol{\sigma} + \sum_{j=0}^i f((\mathcal{F}^\top)^j \boldsymbol{\sigma}, \mathbb{E}\{\tilde{\mathbf{w}}(i-j)\}) \tag{80}$$

where $\tilde{\mathbf{w}}(0) = \mathbf{w}^* - \mathbf{w}(0)$. Provided that \mathcal{F} is stable, the first and second terms on the RHS of (80) converge as $i \rightarrow \infty$, to zero for the former and to a finite value for the latter. Consider the third term. We know from (36) that $\mathbb{E}\{\tilde{\mathbf{w}}(i)\}$ is uniformly bounded because (36) is a Bounded Input Bounded Output (BIBO) stable recursion with a bounded driving term $\eta \mathcal{A}^\top \mathcal{M} \mathcal{Q} \mathbf{w}^*$. We know that for every square matrix \mathbf{X} and every $\epsilon > 0$, there exists a submultiplicative norm $\|\cdot\|_{\rho}$ such that $\|\mathbf{X}\|_{\rho} = \rho(\mathbf{X}) + \epsilon$ [43]. Since the matrix \mathcal{F}^\top is stable, then we can find an $\epsilon > 0$ such that $\|\mathcal{F}^\top\|_{\rho} = \rho(\mathcal{F}^\top) + \epsilon = c_{\rho} < 1$. Applying this norm to \mathbf{f} , we obtain:

$$\begin{aligned}
\|f((\mathcal{F}^\top)^j \boldsymbol{\sigma}, \mathbb{E}\{\tilde{\mathbf{w}}(i-j)\})\|_{\rho} &= \|\eta^2 \mathbf{r}_b^\top (\mathcal{F}^\top)^j \boldsymbol{\sigma} + 2\eta \mathbb{E}\{\tilde{\mathbf{w}}(i-j)\}^\top \mathbf{K}^\top (\mathcal{F}^\top)^j \boldsymbol{\sigma}\|_{\rho} \\
&\leq \eta^2 \|\mathbf{r}_b^\top (\mathcal{F}^\top)^j \boldsymbol{\sigma}\|_{\rho} + 2\eta \|\mathbb{E}\{\tilde{\mathbf{w}}(i-j)\}^\top \mathbf{K}^\top (\mathcal{F}^\top)^j \boldsymbol{\sigma}\|_{\rho}. \tag{81}
\end{aligned}$$

We then conclude that

$$\|f((\mathcal{F}^\top)^j \boldsymbol{\sigma}, \mathbb{E}\{\tilde{\mathbf{w}}(i-j)\})\|_{\rho} < v c_{\rho}^j \tag{82}$$

for some positive finite constant v . It follows that the sum in the third term on the RHS of (80) converges as $i \rightarrow \infty$. As a result, $\mathbb{E}\{\|\tilde{\mathbf{w}}(i+1)\|_{\sigma}^2\}$ converges to a bounded value as $i \rightarrow \infty$, and the algorithm is mean-square stable.

The stability of \mathcal{F} is studied in Appendix B. ■

Theorem 3. (*Transient network performance*) Consider sufficiently small step-sizes that ensure mean and mean-square stability. The variance curve defined by $\zeta(i) = \mathbb{E}\{\|\tilde{\mathbf{w}}(i+1)\|_{\sigma}^2\}$ evolves according to the following recursion for $i \geq 0$:

$$\zeta(i+1) = \zeta(i) + \mathbf{g}_b^{\top} (\mathcal{F}^{\top})^i \boldsymbol{\sigma} - \|\tilde{\mathbf{w}}(0)\|_{(\mathbf{I}_{(NL)^2} - \mathcal{F}^{\top})(\mathcal{F}^{\top})^i \boldsymbol{\sigma}}^2 + \eta^2 \mathbf{r}_b^{\top} (\mathcal{F}^{\top})^i \boldsymbol{\sigma} + 2\eta \mathbb{E}\{\tilde{\mathbf{w}}(i)\}^{\top} \mathbf{K}^{\top} \boldsymbol{\sigma} + 2\eta \boldsymbol{\Gamma}(i) \boldsymbol{\sigma} \quad (83)$$

where $\boldsymbol{\Gamma}(i+1)$ is updated as follows:

$$\boldsymbol{\Gamma}(i+1) = \boldsymbol{\Gamma}(i) \mathcal{F}^{\top} + \mathbb{E}\{\tilde{\mathbf{w}}(i)\}^{\top} \mathbf{K}^{\top} (\mathcal{F}^{\top} - \mathbf{I}_{(NL)^2}), \quad (84)$$

with the initial conditions $\zeta(0) = \|\tilde{\mathbf{w}}(0)\|_{\sigma}^2$ and $\boldsymbol{\Gamma}(0) = \mathbf{0}_{(NL)^2}^{\top}$. The network mean-square deviation (MSD) is obtained by setting $\boldsymbol{\sigma} = \text{bvec}(\boldsymbol{\Sigma})$ with $\boldsymbol{\Sigma} = \frac{1}{N} \mathbf{I}_{NL}$.

Proof: The argument is similar to the proof of Theorem 3 in [26]. ■

Theorem 4. (*Steady-state network performance*) Assume sufficiently small step-sizes to ensure mean and mean-square convergence. Then, the steady-state performance for multitask diffusion LMS (9) applied to asynchronous network is given by:

$$\zeta^* = \mathbf{g}_b^{\top} (\mathbf{I}_{(NL)^2} - \mathcal{F}^{\top})^{-1} \boldsymbol{\sigma} + f((\mathbf{I}_{(NL)^2} - \mathcal{F}^{\top})^{-1} \boldsymbol{\sigma}, \mathbb{E}\{\tilde{\mathbf{w}}(\infty)\}). \quad (85)$$

where $\mathbb{E}\{\tilde{\mathbf{w}}(\infty)\}$ is given by (45). The network mean-square deviation (MSD) is obtained by setting $\boldsymbol{\sigma} = \text{bvec}(\boldsymbol{\Sigma})$ with $\boldsymbol{\Sigma} = \frac{1}{N} \mathbf{I}_{NL}$.

Proof: The steady-state network performance with metric $\boldsymbol{\sigma}$ is defined as:

$$\zeta^* = \lim_{i \rightarrow \infty} \mathbb{E}\{\|\tilde{\mathbf{w}}(i)\|_{\sigma}^2\}. \quad (86)$$

From the recursive expression (79), we obtain as $i \rightarrow \infty$:

$$\lim_{i \rightarrow \infty} \mathbb{E}\{\|\tilde{\mathbf{w}}(i)\|_{(\mathbf{I}_{(NL)^2} - \mathcal{F}^{\top}) \boldsymbol{\sigma}}^2\} = \mathbf{g}_b^{\top} \boldsymbol{\sigma} + f(\boldsymbol{\sigma}, \mathbb{E}\{\tilde{\mathbf{w}}(\infty)\}). \quad (87)$$

To obtain (86), we replace $\boldsymbol{\sigma}$ in (87) by $(\mathbf{I}_{(NL)^2} - \mathcal{F}^{\top})^{-1} \boldsymbol{\sigma}$. ■

Before moving on to the presentation of experimental results, note that the performance of the *synchronous* multitask algorithm over the *mean-graph* topology can be obtained by setting C_A , C_M and C_P to zero in (60)–(62).

IV. SIMULATION RESULTS

A. Illustrative example

We adopt the same clustered multitask network as [26] in our simulations. As shown in Figure 2, the network consists of 10 nodes divided into 4 clusters: $\mathcal{C}_1 = \{1, 2, 3\}$, $\mathcal{C}_2 = \{4, 5, 6\}$, $\mathcal{C}_3 = \{7, 8\}$, $\mathcal{C}_4 = \{9, 10\}$. The unknown parameter vector $\mathbf{w}_{\mathcal{C}_i}^*$ of each cluster is of size 2×1 , and has the following form: $\mathbf{w}_{\mathcal{C}_i}^* = \mathbf{w}_0 + \delta\mathbf{w}_{\mathcal{C}_i}$ with $\mathbf{w}_0 = [0.5, -0.4]^\top$, $\delta\mathbf{w}_{\mathcal{C}_1} = [0.0287, -0.005]^\top$, $\delta\mathbf{w}_{\mathcal{C}_2} = [0.0234, 0.005]^\top$, $\delta\mathbf{w}_{\mathcal{C}_3} = [-0.0335, 0.0029]^\top$, and $\delta\mathbf{w}_{\mathcal{C}_4} = [0.0224, 0.00347]^\top$. The input and output data at each node k are related via the linear regression model: $d_k(i) = \mathbf{x}_k^\top(i)\mathbf{w}_k^* + z_k(i)$ where $\mathbf{w}_k^* = \mathbf{w}_{\mathcal{C}(k)}^*$. The regressors are zero-mean 2×1 random vectors governed by a Gaussian distribution with covariance matrices $\mathbf{R}_{x,k} = \sigma_{x,k}^2 \mathbf{I}_L$. The variances $\sigma_{x,k}^2$ are shown in Figure 2. The background noises $z_k(i)$ are independent and identically distributed zero-mean Gaussian random variables, independent of any other signals. The corresponding variances are given in Figure 2.

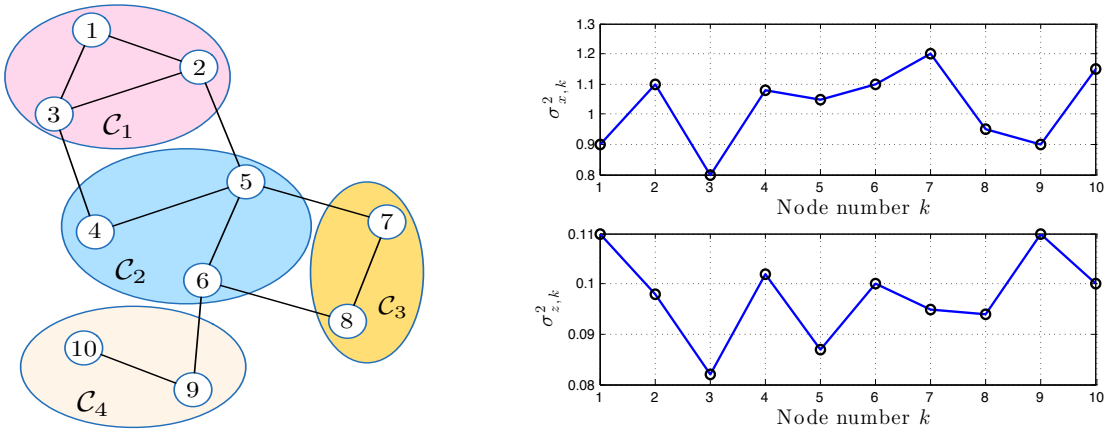


Fig. 2. Experimental setup. Left: Network topology. Right: Regression and noise variances.

We considered the Bernoulli asynchronous model described in Appendix A. We set the coefficient $a_{\ell k}$ in (95) such that $a_{\ell k} = |\mathcal{N}_k \cap \mathcal{C}(k)|^{-1}$ for all $\ell \in (\mathcal{N}_k \cap \mathcal{C}(k))$, where $|\mathcal{N}_k \cap \mathcal{C}(k)|$ denotes the cardinality of the set $\mathcal{N}_k \cap \mathcal{C}(k)$. Then we set the regularization factors $\rho_{k\ell}$ in (99) as follows. If $\mathcal{N}_k \setminus \mathcal{C}(k) \neq \emptyset$, $\rho_{k\ell}$ was set to $\rho_{k\ell} = |\mathcal{N}_k \setminus \mathcal{C}(k)|^{-1}$ for all $\ell \in \mathcal{N}_k \setminus \mathcal{C}(k)$, and to $\rho_{k\ell} = 0$ for any other ℓ . If $\mathcal{N}_k \setminus \mathcal{C}(k) = \emptyset$, these factors were set to $\rho_{kk} = 1$ and to $\rho_{k\ell} = 0$ for all $\ell \neq k$. This usually leads to asymmetrical regularization factors. The parameters of the Bernoulli distribution governing the step-sizes $\mu_k(i)$ were the same over the network, that is, we set μ_k in (93) to 0.03 for all k . The regularization strength η was set to 1. The MSD learning curves were averaged over 100 Monte-Carlo runs. The transient MSD curves were obtained with Theorem 3, and the steady-state MSD was estimated with Theorem 4. In Figure 3 (left), we report the network MSD learning curves for 3 different cases:

- 1) 50% idle: $q_k = p_{\ell k} = r_{k\ell} = 0.5$;
- 2) 30% idle: $q_k = p_{\ell k} = r_{k\ell} = 0.7$;
- 3) no idle nodes: $q_k = p_{\ell k} = r_{k\ell} = 1$.

We observe that the simulation results match well the theoretical results. Furthermore, the performance of the network is influenced by the probability of occurrence of random events. In Figure 3 (right), the asynchronous algorithm in Case 2) is compared with its synchronous version obtained from (7) by setting μ_k , $a_{\ell k}$, and $\rho_{k\ell}$ to the expected values $\bar{\mu}_k = \mathbb{E}\{\mu_k(i)\}$, $\bar{a}_{\ell k} = \mathbb{E}\{a_{\ell k}(i)\}$, and $\bar{\rho}_{k\ell} = \mathbb{E}\{\rho_{k\ell}(i)\}$, respectively. Although both algorithms show the same convergence rate, the asynchronous algorithm suffers from degradation in its MSD performance caused by the additional randomness throughout the adaptation process.

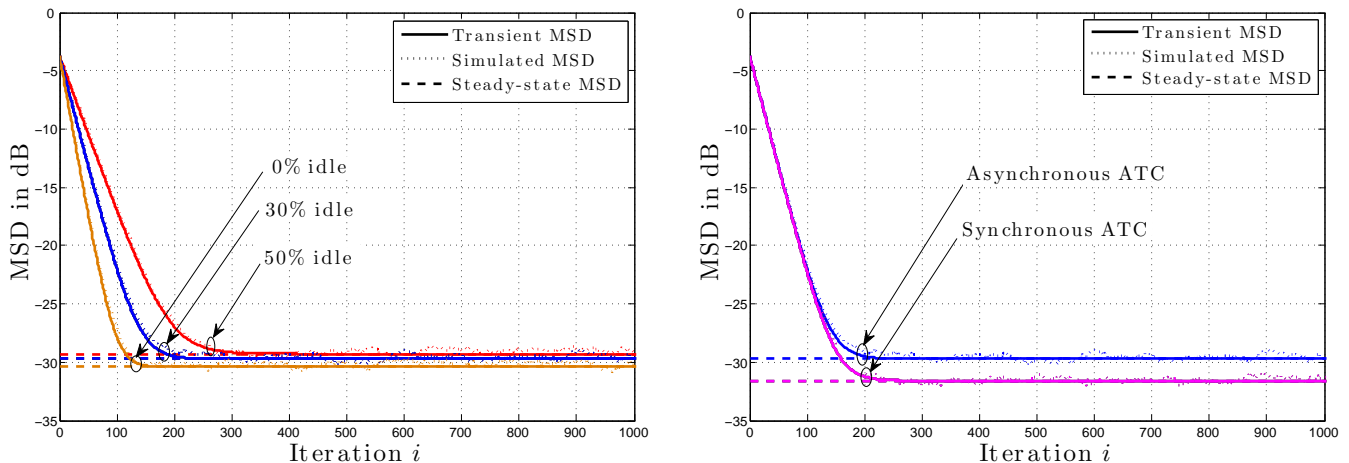


Fig. 3. Left: Comparison of asynchronous network MSD under 50% idle, 30% idle, and 0% idle. Right: Network MSD comparison of asynchronous network under 30% idle and the corresponding synchronous network.

B. Multitask learning benefit

In this section we provide an example to show the benefit of multitask learning. We consider a network consisting of $N = 21$ nodes grouped into $Q = 3$ clusters as shown in Figure 4. The inputs $\mathbf{x}_k(i)$ were zero-mean 9×1 random vectors governed by a Gaussian distribution with covariance matrix $\mathbf{R}_{x,k} = \sigma_{x,k}^2 \mathbf{I}_9$, with $\sigma_{x,k}^2$ shown in Figure 4. The noises $z_k(i)$ were i.i.d. zero-mean Gaussian random variables, independent of any other signal with variances $\sigma_{z,k}^2$ shown in Figure 4. The 9×1 unknown parameter vectors were chosen as: $\mathbf{w}_{\mathcal{C}_1}^* = \mathbf{w}_0 = [1 \ 1 \ 1 \ 0 \ 0 \ 0 \ 2 \ 2 \ 2]$, $\mathbf{w}_{\mathcal{C}_2}^* = \mathbf{w}_0 + \delta\mathbf{w}$, $\mathbf{w}_{\mathcal{C}_3}^* = \mathbf{w}_0 - \delta\mathbf{w}$ where $\delta\mathbf{w} = [0.01 \ -0.01 \ 0.02 \ -0.02 \ 0 \ 0 \ 0.01 \ -0.01 \ 0]$.

We considered the Bernoulli asynchronous model. The coefficients $\{a_{\ell k}\}$ and $\{\rho_{k\ell}\}$ in (95) and (99), respectively, were generated in the same manner as in IV-A. Parameters μ_k and q_k in (93) were set to $\mu_k = 1/30$, $q_k = 0.8$ for nodes in the first cluster, $\mu_k = 2/45$, $q_k = 0.6$ for nodes in the second cluster, and $\mu_k = 1/15$, $q_k = 0.4$ for nodes in the third cluster. The probabilities $\{p_{\ell k}\}$ in (95) were $p_{\ell k} = 0.8$ for links in the first cluster, $p_{\ell k} = 0.6$ for links in the second cluster, and $p_{\ell k} = 0.4$ for links in the third cluster. The probability that a link connecting two nodes belonging to neighboring clusters drops was $1 - r_{k\ell} = 0.25$. The simulated curves were obtained by averaging over 100 Monte-Carlo runs.

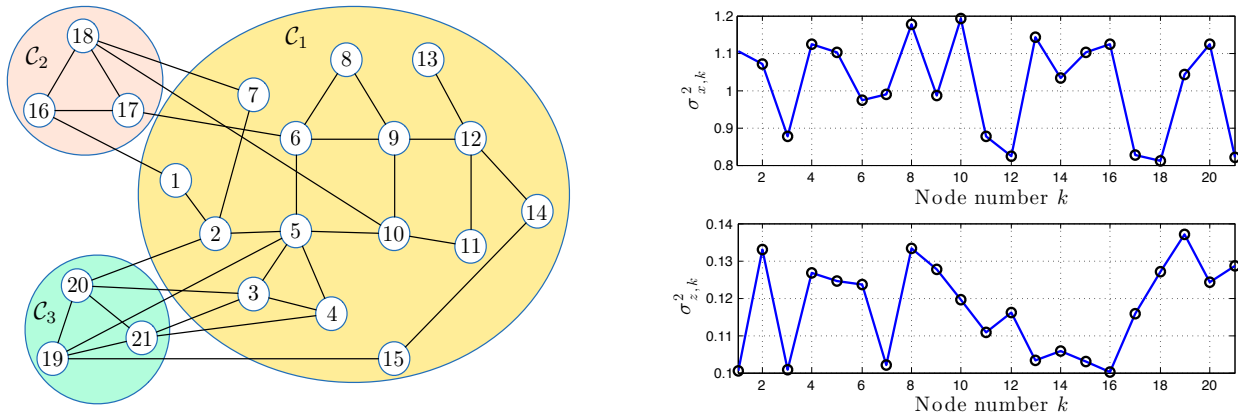


Fig. 4. Experimental setup. Left: Network topology. Right: Regression and noise variances.

In Figure 5 (left), we compare two algorithms: the asynchronous diffusion strategy without regularization (obtained from (9) by setting $\eta = 0$) and its synchronous version (obtained from (9) by setting $\eta = 0$ and replacing $\mu_k(i), a_{\ell k}(i)$ by $\bar{\mu}_k, \bar{a}_{\ell k}$). As shown in this figure, the performance is highly deteriorated in the third cluster and slightly deteriorated in the first cluster because \mathcal{C}_3 is more susceptible to random events. In Figure 5 (right), we compare two algorithms: the asynchronous diffusion strategy with regularization (obtained from (9) by setting $\eta = 1$) and the same synchronous algorithm as in the left plot. As shown in this figure, the cooperation between clusters improves well the performance of clusters 2 and 3 so that gaps appearing in the left plot are reduced. In other words, \mathcal{C}_2 and \mathcal{C}_3 benefit from the high performance levels achieved by \mathcal{C}_1 that can be justified by two arguments: a large number of nodes is employed to collectively estimate $w_{\mathcal{C}_1}^*$ and the probabilities associated with random events in \mathcal{C}_1 are small. In conclusion, when tasks between neighboring clusters are similar, cooperation among clusters improves the learning especially for clusters where the asynchronous events occur frequently.

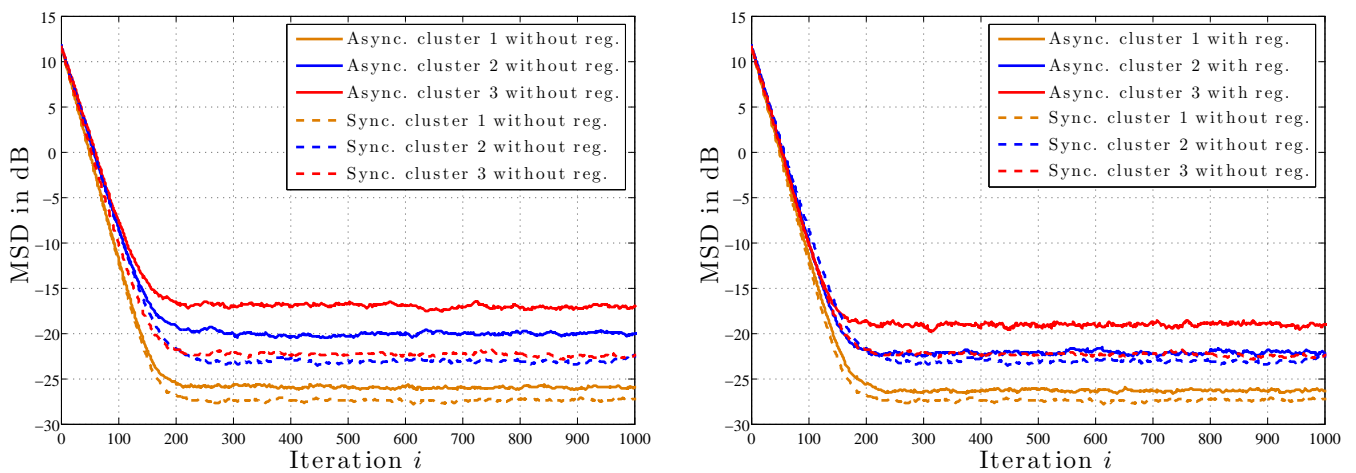


Fig. 5. Clusters learning curves. Left: Comparison of asynchronous network without regularization and its synchronous version. Right: Comparison of asynchronous network with regularization and the synchronous network without regularization.

C. Distributed spectrum sensing

Cognitive radio is a form of wireless communication in which a transceiver can intelligently detect which communication channels are in use and which are not. This allows to optimize the use of available radio frequencies in the spectrum while avoiding causing harmful interference to the licensed users [44]. One of the main functions of cognitive radio is spectrum sensing where each secondary user, that is, unlicensed user, has to detect the frequency bands used by the N_P primary users, that is, licensed users, even under low signal to noise ratio (SNR) conditions. In order to perform this task, each secondary user can estimate the aggregated power spectrum transmitted by all active primary users. Different scenarios were considered in the literature to address this problem in a cooperative manner. The single-task diffusion LMS algorithm was considered in [16], [45], over a communication network consisting of N_S secondary users equipped each with a single antenna device. In [26], each secondary user was considered as a cluster of N_R nodes, where N_R is the number of antennas available for each unlicensed user. The synchronous multitask diffusion LMS algorithm was used to perform the inference task. As illustrated in this work, promoting cooperation among clusters improves the estimation accuracy as well as increasing the number of antennas per user.

Each antenna ℓ of each secondary user k is able to reconstruct the aggregated power spectrum that is transmitted by all active primary users by estimating the vector of $N_B \times N_P$ combination weights $\boldsymbol{\alpha}^* = \text{col}\{\boldsymbol{\alpha}_1, \dots, \boldsymbol{\alpha}_{N_P}\}$ where N_B is the number of basis functions used to represent the power spectrum transmitted by primary users and $\boldsymbol{\alpha}_q = [\alpha_{q1}, \dots, \alpha_{qN_B}]^\top$. Let $\mathbf{r}_{k\ell}(i)$ denote the $N_F \times 1$ vector whose j -th entry $r_{k\ell,j}(i)$ is the measurement of the power spectrum sensed by the pair (k, ℓ) at time instant i and over the frequency f_j . Let $\mathbf{z}_{k\ell}(i)$ denote the $N_F \times 1$ vector containing the N_F noise samples $z_{k\ell,j}(i)$. Furthermore, let us introduce the $N_F \times N_B$ matrix $\boldsymbol{\Phi}$ whose j -th row contains the magnitudes of the N_B basis functions at the frequency sample f_j and let us define the matrix $\boldsymbol{\Phi}_{k\ell}(i) = [p_{1,k\ell}(i), \dots, p_{N_P,k\ell}(i)] \otimes \boldsymbol{\Phi}$ where $p_{q,k\ell}(i)$ is the path loss factor between the primary user q and the ℓ -th antenna of node k at time i . It was shown in [26] that the measurements $\mathbf{r}_{k\ell}(i)$ and $\boldsymbol{\Phi}_{k\ell}(i)$ are related via the linear regression model:

$$\mathbf{r}_{k\ell}(i) = \boldsymbol{\Phi}_{k\ell}(i)\boldsymbol{\alpha}^* + \mathbf{z}_{k\ell}(i). \quad (88)$$

Each pair (k, ℓ) is able to estimate $\boldsymbol{\alpha}^*$ by minimizing a mean-square error criterion without cooperation. However, by considering each multi-antenna device as a cluster of N_R nodes, the multitask diffusion algorithm allows to enhance the estimation accuracy.

Asynchronous events are often encountered in such applications. To show the effect of the randomness at the level of nodes and links, we considered a cognitive radio system consisting of $N_P = 3$ primary users and $N_S = 10$ secondary users. Each secondary user was equipped with $N_R = 4$ antennas. We assumed that each cluster was fully connected. The network topology is shown in Figure 6. The power spectrum transmitted by the primary user q was represented by a combination of $N_B = 21$ Gaussian basis functions centered at the normalized frequency

f_m with variance $\sigma_m^2 = 0.001$ for all m :

$$\phi_m(f) = e^{-\frac{(f-f_m)^2}{2\sigma_m^2}}. \quad (89)$$

The central frequencies f_m were uniformly distributed along the frequency axis. We set the combination vectors α_j^* as follows:

$$\begin{aligned} \alpha_1^* &= [\mathbf{0}_{1 \times 2} \ 0.3 \ 0.28 \ 0.3 \ \mathbf{0}_{1 \times 15}]^\top \\ \alpha_2^* &= [\mathbf{0}_{1 \times 9} \ 0.3 \ 0.3 \ \mathbf{0}_{1 \times 9}]^\top \\ \alpha_3^* &= [\mathbf{0}_{1 \times 15} \ 0.3 \ 0.28 \ 0.3 \ \mathbf{0}_{1 \times 2}]^\top. \end{aligned} \quad (90)$$

Each secondary user got measurements of the received signal over $N_F = 80$ frequency bands. Based on the free space propagation theory, we set $\bar{p}_{q,k}$ to the inverse of the squared distance between the transmitter q and the receiver k . At each time instant i , the path loss factor between the pair (k, ℓ) and the primary user q was set to

$$p_{q,k\ell}(i) = \bar{p}_{q,k} + \delta p_{q,k\ell}(i) \quad (91)$$

with $\delta p_{q,k\ell}(i)$ a zero-mean random Gaussian variable with standard deviation $0.1 \bar{p}_{q,k}$. The ℓ -th node of the secondary user k estimated the path loss factors according to the following model:

$$\hat{p}_{q,k\ell}(i) = \begin{cases} \bar{p}_{q,k}, & \text{if } p_{q,k\ell}(i) > p_0, \\ 0, & \text{otherwise} \end{cases} \quad (92)$$

with p_0 a threshold value. The sampling noise $z_{k\ell,j}(i)$ was assumed to be a zero-mean random Gaussian variable with standard deviation 0.01.

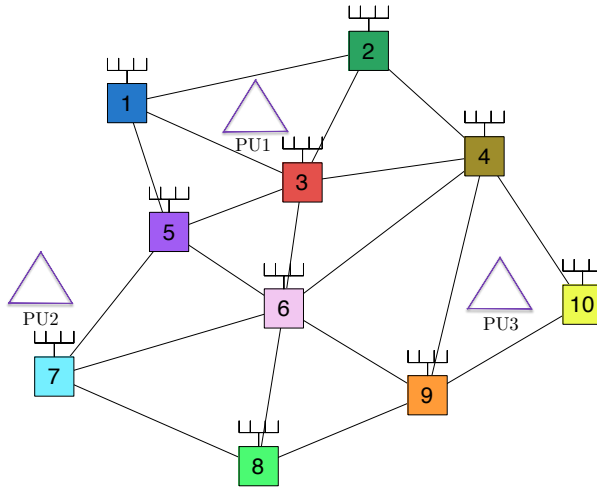


Fig. 6. A cognitive radio system of 3 primary users and 10 secondary users each equipped with 4 antennas.

We considered a Bernoulli asynchronous model. The coefficient $a_{\ell k}$ in (95) was set to $\frac{1}{N_R}$ if it corresponds to an intra-cluster link and to zero otherwise. We also used uniform regularization factors ρ_{st} in (99), that is, the regularization factor between pairs $s = (k, \ell)$ and $t = (m, n)$ of neighboring clusters was set to $\frac{1}{N_R \times |\mathcal{N}_k|}$, with $|\mathcal{N}_k|$ the number of neighboring secondary users of user k . The probability of success associated with the step-size

parameter $\mu_{k\ell}(i)$ was uniform for all pairs (k, ℓ) and equal to 0.4, that is, the probability that an antenna does not work at a given time i was 0.6. The probability of success associated with intra-cluster links was 0.4 for all pairs (k, ℓ) and (m, n) belonging to the same cluster. However, we allowed the probability of success associated with links connecting two nodes belonging to different clusters to be space dependent. We denote by $p_{k\ell, mn}$ the probability that the link connecting the ℓ -th antenna of user k to the n -th antenna of the neighboring user m works at a time instant i , and $d(k, m)$ the distance between these neighboring users. For our experiments, we set the probability $p_{k\ell, mn}$ to $e^{-a \cdot d(k, m)}$ for $\ell, n = 1, \dots, N_R$ where we chose $a = 0.15$.

The MSD learning curves were averaged over 50 Monte-Carlo runs. We ran the synchronous and asynchronous multitask algorithms in two different situations. For the first one, we set the regularization strength η to zero, that is, we did not allow any cooperation between neighboring clusters. In the second one, we set the regularization strength η to 0.015. Note that the synchronous algorithm is obtained from the asynchronous algorithm by making the random step-size $\mu_{k\ell}(i)$ a deterministic quantity equal to $\bar{\mu}_{k\ell}$, the random combination coefficient $a_{mn, k\ell}(i)$ (likewise the regularization coefficient $\rho_{k\ell, mn}(i)$) between the pairs (k, ℓ) and (m, n) a deterministic quantity equal to $\bar{a}_{mn, k\ell}$ (likewise $\bar{\rho}_{k\ell, mn}$). Figure 7 shows that the network MSD performance is significantly improved through cooperation among clusters. Furthermore, it is worth noting that the degradation is minimal and that the network still deliver performance despite the asynchronous events. In other words, the diffusion adaptation endows networks with robustness towards asynchronous events. Figure 8 depicts the estimated power spectrum density for nodes 4, 6 and 10. The result on the left can be interpreted based on the distance between primary and secondary users, which leads to hidden node effects. With cooperation between neighboring secondary users, regardless of the distance between primary and secondary users, each secondary user was able to estimate the aggregated power spectrum transmitted by all active primary users. It can be observed that there is no difference between the estimated PSD in synchronous and asynchronous situations.

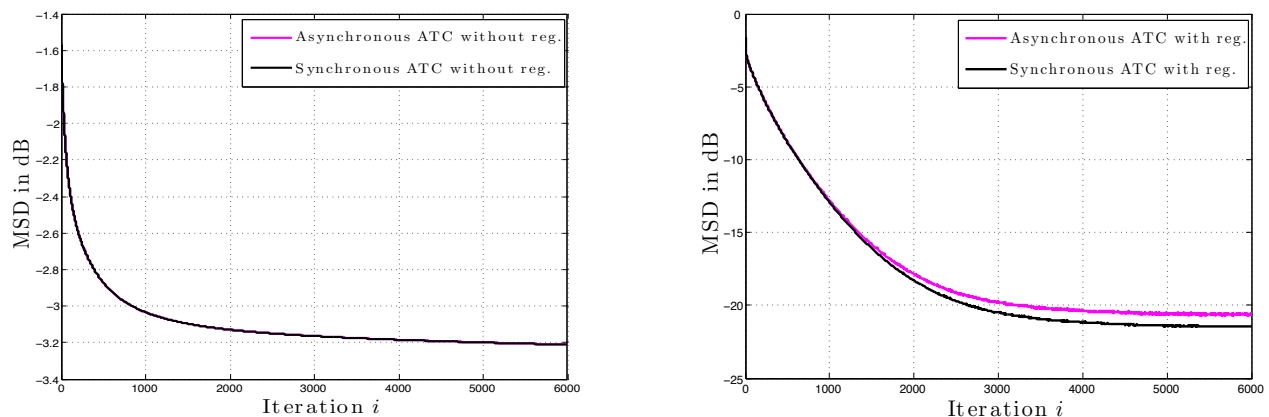


Fig. 7. MSD learning curves for synchronous and asynchronous networks. Left: non-cooperative devices. Right: cooperative devices.

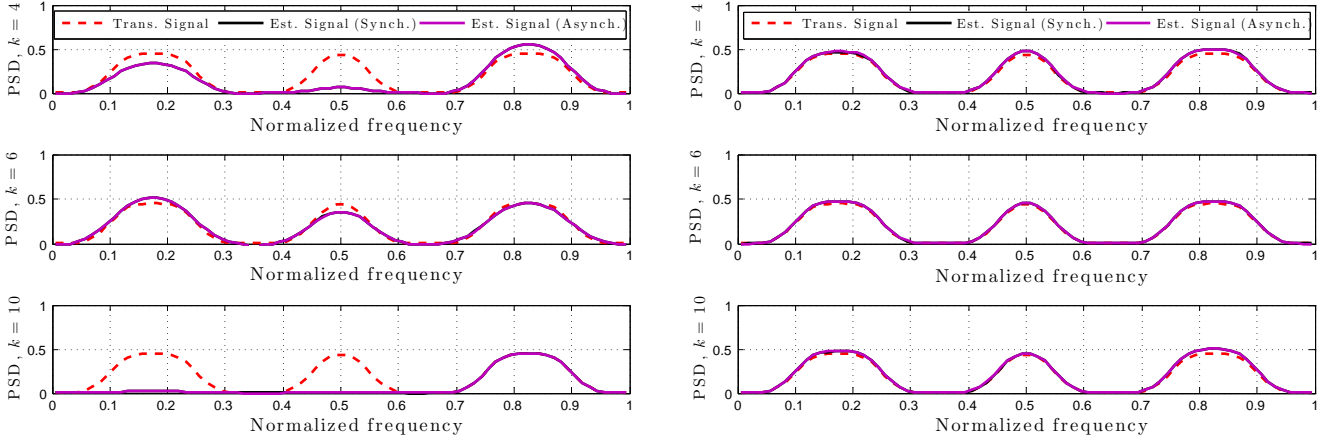


Fig. 8. PSD estimation in synchronous and asynchronous networks for nodes 4, 6 and 10. Left: non-cooperative devices. Right: Cooperative devices.

V. CONCLUSION AND PERSPECTIVES

In this paper, we considered multitask problems where networks are able to handle situations beyond the case where the nodes estimate a unique parameter vector over the network. We introduced a general model for asynchronous behavior with random step-sizes, combination coefficients and co-regularization factors. We then carried out a convergence analysis of the asynchronous multitask algorithm in the mean and mean-square-error sense, and we derived conditions for convergence. Several open problems still have to be solved for specific applications. For instance, it would be interesting to investigate how nodes can autonomously adjust co-regularization factors between neighboring clusters in order to optimize the learning performance. It would also be advantageous to consider alternative co-regularizers in order to promote properties such as sparsity or block sparsity, and to analyze the convergence behavior of the resulting algorithms.

APPENDIX A

THE BERNOULLI MODEL

In this model, the step-sizes $\{\mu_k(i)\}$ are distributed as follows:

$$\mu_k(i) = \begin{cases} \mu_k, & \text{with probability } q_k \\ 0, & \text{with probability } 1 - q_k \end{cases} \quad (93)$$

where μ_k is a fixed value. This probability distribution allows us to model random “on-off” behavior by each agent k due to power saving strategies or random agent failures. We assume that the step-sizes $\mu_k(i)$ are spatially uncorrelated for different k . At each iteration i , the mean of the step-size $\mu_k(i)$ is $\bar{\mu}_k = \mu_k q_k$, and the covariance between $\mu_k(i)$ and $\mu_\ell(i)$ is:

$$c_{\mu,k,\ell} \triangleq \mathbb{E}\{(\mu_k(i) - \bar{\mu}_k)(\mu_\ell(i) - \bar{\mu}_\ell)\} = \begin{cases} \mu_k^2 q_k (1 - q_k), & \text{if } \ell = k \\ 0, & \text{otherwise.} \end{cases} \quad (94)$$

Furthermore, combination weights $\{a_{\ell k}(i)\}$ are distributed as follows:

$$a_{\ell k}(i) = \begin{cases} a_{\ell k}, & \text{with probability } p_{\ell k} \\ 0, & \text{with probability } 1 - p_{\ell k} \end{cases} \quad (95)$$

for any $\ell \in \mathcal{N}_k^-(i) \cap \mathcal{C}(k)$, where $0 < a_{\ell k} < 1$ a fixed coefficient. The coefficients $\{a_{\ell k}(i)\}$ are spatially uncorrelated for different ℓ and k . Node k adjusts its own combination coefficient to ensure that the sum of its neighboring coefficients is equal to one as follows:

$$a_{kk}(i) = 1 - \sum_{\ell \in \mathcal{N}_k^-(i) \cap \mathcal{C}(k)} a_{\ell k}(i) \geq 0. \quad (96)$$

The probability distribution (95) allows us to model a random ‘‘on-off’’ status for links within clusters at time i due to communication cost saving strategies or random link failures. With this model, we are giving the opportunity to each agent k to randomly choose a subset of neighbors that belong to its cluster to perform the combination step. At each iteration i , the mean of the coefficient $a_{\ell k}(i)$ is given by:

$$\bar{a}_{\ell k} = \begin{cases} a_{\ell k} p_{\ell k}, & \text{if } \ell \in \mathcal{N}_k^- \cap \mathcal{C}(k) \\ 1 - \sum_{\ell \in \mathcal{N}_k^- \cap \mathcal{C}(k)} a_{\ell k} p_{\ell k}, & \text{if } \ell = k \\ 0, & \text{otherwise.} \end{cases} \quad (97)$$

and the covariance between $a_{\ell k}(i)$ and $a_{nm}(i)$ equals [35]:

$$c_{a,\ell k, nm} = \mathbb{E}\{(a_{\ell k}(i) - \bar{a}_{\ell k})(a_{nm}(i) - \bar{a}_{nm})\} = \begin{cases} c_{a,\ell k, \ell k}, & \text{if } k = m, \ell = n, \ell \in \mathcal{N}_k^- \cap \mathcal{C}(k) \\ -c_{a,\ell k, \ell k}, & \text{if } k = m = n, \ell \in \mathcal{N}_k^- \cap \mathcal{C}(k) \\ -c_{a,nk, nk}, & \text{if } k = m = \ell, n \in \mathcal{N}_k^- \cap \mathcal{C}(k) \\ \sum_{j \in \mathcal{N}_k^- \cap \mathcal{C}(k)} c_{a,jk, jk}, & \text{if } k = m = \ell = n \\ 0, & \text{otherwise.} \end{cases} \quad (98)$$

where $c_{a,\ell k, \ell k} = a_{\ell k}^2 p_{\ell k} (1 - p_{\ell k})$.

Finally, the regularization factors $\{\rho_{k\ell}(i)\}$ are distributed as follows:

$$\rho_{k\ell}(i) = \begin{cases} \rho_{k\ell}, & \text{with probability } r_{k\ell} \\ 0, & \text{with probability } 1 - r_{k\ell} \end{cases} \quad (99)$$

for any $\ell \in \mathcal{N}_k(i) \setminus \mathcal{C}(k)$, where $0 < \rho_{k\ell} < 1$ is a fixed regularization factor. The factors $\{\rho_{k\ell}(i)\}$ are spatially uncorrelated for $k \neq \ell$. At each iteration i , in order to get a right stochastic matrix $\mathbf{P}(i)$, node k adjusts its regularization factor as follows:

$$\rho_{kk}(i) = 1 - \sum_{\ell \in \mathcal{N}_k(i) \setminus \mathcal{C}(k)} \rho_{k\ell}(i) \geq 0. \quad (100)$$

The probability distribution (99) allows each agent k to randomly select a subset of neighbors that do not belong to its cluster and introduce co-regularization in the estimation process. This behavior can also be interpreted as

resulting from link random failures between neighboring clusters: at every time instant i , the communication link from agent ℓ to agent k drops with probability $1 - r_{k\ell}$. The mean of $\rho_{k\ell}(i)$ is given:

$$\bar{\rho}_{k\ell} = \begin{cases} \rho_{k\ell} r_{k\ell}, & \text{if } \ell \in \mathcal{N}_k \setminus \mathcal{C}(k) \\ 1 - \sum_{\ell \in \mathcal{N}_k \setminus \mathcal{C}(k)} \rho_{k\ell} r_{k\ell}, & \text{if } \ell = k \\ 0, & \text{otherwise,} \end{cases} \quad (101)$$

and the covariance between $\rho_{k\ell}(i)$ and $\rho_{mn}(i)$ is:

$$c_{\rho,k\ell,mn} = \mathbb{E}\{(\rho_{k\ell}(i) - \bar{\rho}_{k\ell})(\rho_{mn}(i) - \bar{\rho}_{mn})\} = \begin{cases} c_{\rho,k\ell,k\ell}, & \text{if } k = m, \ell = n, \ell \in \mathcal{N}_k \setminus \mathcal{C}(k) \\ -c_{\rho,k\ell,k\ell}, & \text{if } k = m = n, \ell \in \mathcal{N}_k \setminus \mathcal{C}(k) \\ -c_{\rho,kn,kn}, & \text{if } k = m = \ell, n \in \mathcal{N}_k \setminus \mathcal{C}(k) \\ \sum_{j \in \mathcal{N}_k \setminus \mathcal{C}(k)} c_{\rho,kj,kj}, & \text{if } k = m = \ell = n \\ 0, & \text{otherwise} \end{cases} \quad (102)$$

where $c_{\rho,k\ell,k\ell} = \rho_{k\ell}^2 r_{k\ell} (1 - r_{k\ell})$.

APPENDIX B

STABILITY OF \mathcal{F}

Recall from (69) that

$$\mathcal{F} = \mathcal{A}_I^\top [I_{(NL)^2} - I_{NL} \otimes_b \mathcal{M}(\mathcal{R}_x + \eta \mathcal{Q}) - \mathcal{M}(\mathcal{R}_x + \eta \mathcal{Q}) \otimes_b I_{NL}]. \quad (103)$$

We now upper-bound the spectral radius of \mathcal{F} in order to derive a sufficient condition for mean-square stability of the algorithm. We can write:

$$\rho(\mathcal{F}) \leq \|\mathcal{A}_I^\top\|_{b,\infty} \cdot \|I_{(NL)^2} - I_{NL} \otimes_b \mathcal{M}(\mathcal{R}_x + \eta \mathcal{Q}) - \mathcal{M}(\mathcal{R}_x + \eta \mathcal{Q}) \otimes_b I_{NL}\|_{b,\infty} \quad (104)$$

Since the matrix \mathcal{A}_I is a block left-stochastic matrix, we know that $\|\mathcal{A}_I^\top\|_{b,\infty} = 1$. Using (43) and the triangular inequality, we have:

$$\begin{aligned} \rho(\mathcal{F}) &\leq \|I_{(NL)^2} - I_{NL} \otimes_b \mathcal{M}(\mathcal{R}_x + \eta I_{NL}) - \mathcal{M}(\mathcal{R}_x + \eta I_{NL}) \otimes_b I_{NL}\|_{b,\infty} + \\ &\quad \eta \|I_{NL} \otimes_b \mathcal{M}\mathcal{P}\|_{b,\infty} + \eta \|\mathcal{M}\mathcal{P} \otimes_b I_{NL}\|_{b,\infty}. \end{aligned} \quad (105)$$

Consider the second term on the RHS of (105). We know that

$$\begin{aligned} I_{NL} \otimes_b \mathcal{M}\mathcal{P} &\stackrel{(55)}{=} (I_{NL} \otimes_b \mathcal{M})(I_{NL} \otimes_b \mathcal{P}) \\ &\stackrel{(56)}{=} \left((I_N \otimes \bar{\mathbf{M}}) \otimes I_{L^2} \right) \left((I_N \otimes \bar{\mathbf{P}}) \otimes I_{L^2} \right). \end{aligned} \quad (106)$$

Since $\left((I_N \otimes \bar{\mathbf{P}}) \otimes I_{L^2} \right)$ is a block right-stochastic matrix and $\left((I_N \otimes \bar{\mathbf{M}}) \otimes I_{L^2} \right)$ is an $N^2 \times N^2$ block diagonal matrix with each block of the form $\bar{\mu}_k I_{L^2}$ ($k = 1, \dots, N$), we obtain:

$$\begin{aligned} \|I_{NL} \otimes_b \mathcal{M}\mathcal{P}\|_{b,\infty} &\leq \|(I_N \otimes \bar{\mathbf{M}}) \otimes I_{L^2}\|_{b,\infty} \cdot \|(I_N \otimes \bar{\mathbf{P}}) \otimes I_{L^2}\|_{b,\infty} \\ &= \max_{1 \leq k \leq N} \bar{\mu}_k \end{aligned} \quad (107)$$

Following the same steps for the third term on the RHS of (105), we have:

$$\|\mathcal{MP} \otimes_b \mathbf{I}_{NL}\|_{b,\infty} \leq \max_{1 \leq k \leq N} \bar{\mu}_k. \quad (108)$$

The matrix $[\mathbf{I}_{(NL)^2} - \mathbf{I}_{NL} \otimes_b \mathcal{M}(\mathbf{R}_x + \eta \mathbf{I}_{NL}) - \mathcal{M}(\mathbf{R}_x + \eta \mathbf{I}_{NL}) \otimes_b \mathbf{I}_{NL}]$ in the first term on the RHS of (105) is an $N^2 \times N^2$ block diagonal matrix. The m -th block on the diagonal (where $m = (\ell - 1)N + k$ for $k, \ell = 1, \dots, N$) is of size $L^2 \times L^2$, symmetric, and has the following form:

$$\begin{aligned} & \mathbf{I}_{L^2} - \mathbf{I}_L \otimes \bar{\mu}_k(\mathbf{R}_{x,k} + \eta \mathbf{I}_L) - \bar{\mu}_\ell(\mathbf{R}_{x,\ell} + \eta \mathbf{I}_L) \otimes \mathbf{I}_L \\ & = (-\bar{\mu}_\ell \mathbf{R}_{x,\ell} - \eta \bar{\mu}_\ell \mathbf{I}_L) \otimes \mathbf{I}_L + \mathbf{I}_L \otimes (\mathbf{I}_L - \bar{\mu}_k \mathbf{R}_{x,k} - \eta \bar{\mu}_k \mathbf{I}_L) \end{aligned} \quad (109)$$

Before proceeding, let us recall the Kronecker sum operator, denoted by \oplus . If \mathbf{A} and \mathbf{B} are two matrices of dimension $L \times L$ each, then

$$\mathbf{A} \oplus \mathbf{B} \triangleq \mathbf{A} \otimes \mathbf{I}_L + \mathbf{I}_L \otimes \mathbf{B}. \quad (110)$$

Let $\lambda_k\{\cdot\}$ denote the k -th eigenvalue of its matrix argument. Then, the eigenvalues of $\mathbf{A} \oplus \mathbf{B}$ are of the form $\lambda_i\{\mathbf{A}\} + \lambda_j\{\mathbf{B}\}$ for $i, j = 1, \dots, L$ [46]. Note that the RHS of equation (109) can be written as

$$(-\bar{\mu}_\ell \mathbf{R}_{x,\ell} - \eta \bar{\mu}_\ell \mathbf{I}_L) \oplus (\mathbf{I}_L - \bar{\mu}_k \mathbf{R}_{x,k} - \eta \bar{\mu}_k \mathbf{I}_L) \quad (111)$$

and its eigenvalues are therefore of the form:

$$1 - \eta \bar{\mu}_k - \bar{\mu}_k \lambda_j\{\mathbf{R}_{x,k}\} - \eta \bar{\mu}_\ell - \bar{\mu}_\ell \lambda_i\{\mathbf{R}_{x,\ell}\} \quad (112)$$

for $i, j = 1, \dots, L$ and $k, \ell = 1, \dots, N$. In order to simplify the mean-square stability condition, we assume that the first order moment of the step-sizes is the same for all nodes. Using the fact that the block maximum norm of a block diagonal Hermitian matrix is equal to the largest spectral radius of its block entries [16], we get:

$$\begin{aligned} & \|\mathbf{I}_{(NL)^2} - \mathbf{I}_{NL} \otimes_b \mathcal{M}(\mathbf{R}_x + \eta \mathbf{I}_{NL}) - \mathcal{M}(\mathbf{R}_x + \eta \mathbf{I}_{NL}) \otimes_b \mathbf{I}_{NL}\|_{b,\infty} \\ & = \max_{1 \leq k, \ell \leq N} \left(\max_{1 \leq i, j \leq L} |1 - 2\eta \bar{\mu} - \bar{\mu}(\lambda_j\{\mathbf{R}_{x,k}\} + \lambda_i\{\mathbf{R}_{x,\ell}\})| \right) \\ & = \max_{1 \leq k, \ell \leq N} \left(\max_{1 \leq i, j \leq L} \{1 - 2\eta \bar{\mu} - \bar{\mu}(\lambda_j\{\mathbf{R}_{x,k}\} + \lambda_i\{\mathbf{R}_{x,\ell}\}), -1 + 2\eta \bar{\mu} + \bar{\mu}(\lambda_j\{\mathbf{R}_{x,k}\} + \lambda_i\{\mathbf{R}_{x,\ell}\})\} \right) \\ & = \max \{1 - 2\eta \bar{\mu} - \bar{\mu} \min_{k,\ell} (\lambda_{\min}\{\mathbf{R}_{x,k}\} + \lambda_{\min}\{\mathbf{R}_{x,\ell}\}), -1 + 2\eta \bar{\mu} + \bar{\mu} \max_{k,\ell} (\lambda_{\max}\{\mathbf{R}_{x,k}\} + \lambda_{\max}\{\mathbf{R}_{x,\ell}\})\} \end{aligned}$$

The minimum (identically the maximum) on k and ℓ that appears in the last equality of (113) is reached for $k = \ell$. Thus, a sufficient condition for mean-square stability is given by:

$$\max_{1 \leq k \leq N} \left(\max_{1 \leq i \leq L} |1 - 2\eta \bar{\mu} - 2\bar{\mu} \lambda_i(\mathbf{R}_{x,k})| + 2\eta \bar{\mu} \right) < 1, \quad (114)$$

which is verified if the first order moment of the step-sizes satisfies:

$$0 < \bar{\mu} < \frac{1}{2\eta + \max_{1 \leq k \leq N} \rho(\mathbf{R}_{x,k})}. \quad (115)$$

REFERENCES

- [1] R. Nassif, C. Richard, A. Ferrari, and A. H. Sayed, "Performance analysis of multitask diffusion adaptation over asynchronous networks," in *Proc. Asilomar Conference on Signals, Systems, and Computers*, Pacific Grove, CA, November 2014.
- [2] A. H. Sayed, "Adaptive networks," *Proc. of the IEEE*, vol. 102, no. 4, pp. 460–497, April 2014.
- [3] A. H. Sayed, "Adaptation, learning, and optimization over networks," *Foundations and Trends in Machine Learning*, vol. 7, no. 4-5, pp. 311–801, July 2014.
- [4] J. Tsitsiklis and M. Athans, "Convergence and asymptotic agreement in distributed decision problems," *IEEE Transactions on Automatic Control*, vol. 29, no. 1, pp. 42–50, January 1984.
- [5] L. Xiao and S. Boyd, "Fast linear iterations for distributed averaging," *System & Control Letters*, vol. 53, no. 9, pp. 65–78, September 2004.
- [6] P. Braca, S. Marano, and V. Matta, "Running consensus in wireless sensor networks," in *Proc. International Conference on Information Fusion (FUSION)*, Cologne, Germany, June-July 2008, pp. 1–6.
- [7] A. Nedic and A. Ozdaglar, "Distributed subgradient methods for multi-agent optimization," *IEEE Transactions on Automatic Control*, vol. 54, no. 1, pp. 48–61, January 2009.
- [8] S. Kar and J. M. F. Moura, "Distributed consensus algorithms in sensor networks with imperfect communication: Link failures and channel noise," *IEEE Transactions on Signal Processing*, vol. 57, no. 1, pp. 355–369, 2009.
- [9] K. Srivastava and A. Nedic, "Distributed asynchronous constrained stochastic optimization," *IEEE Journal of Selected Topics in Signal Processing*, vol. 5, no. 4, pp. 772–790, 2011.
- [10] D. P. Bertsekas, "A new class of incremental gradient methods for least squares problems," *SIAM Journal on Optimization*, vol. 7, no. 4, pp. 913–926, November 1997.
- [11] A. Nedic and D. P. Bertsekas, "Incremental subgradient methods for nondifferentiable optimization," *SIAM Journal on Optimization*, vol. 12, no. 1, pp. 109–138, July 2001.
- [12] M. G. Rabbat and R. D. Nowak, "Quantized incremental algorithms for distributed optimization," *IEEE Journal of Selected Topics in Areas in Communications*, vol. 23, no. 4, pp. 798–808, April 2005.
- [13] D. Blatt, A. O. Hero, and H. Gauchman, "A convergent incremental gradient method with constant step size," *SIAM Journal on Optimization*, vol. 18, no. 1, pp. 29–51, February 2007.
- [14] C. G. Lopes and A. H. Sayed, "Incremental adaptive strategies over distributed networks," *IEEE Transactions on Signal Processing*, vol. 55, no. 8, pp. 4064–4077, August 2007.
- [15] A. H. Sayed, S.-Y. Tu, J. Chen, X. Zhao, and Z. Towfic, "Diffusion strategies for adaptation and learning over networks," *IEEE Signal Processing Magazine*, vol. 30, no. 3, pp. 155–171, May 2013.
- [16] A. H. Sayed, "Diffusion adaptation over networks," in *Academic Press Library in Signal Processing*, R. Chellapa and S. Theodoridis, Eds., vol. 3, pp. 322–454. Elsevier, 2014.
- [17] C. G. Lopes and A. H. Sayed, "Diffusion least-mean squares over adaptive networks: Formulation and performance analysis," *IEEE Transactions on Signal Processing*, vol. 56, no. 7, pp. 3122–3136, July 2008.
- [18] F. S. Cattivelli and A. H. Sayed, "Diffusion LMS strategies for distributed estimation," *IEEE Transactions on Signal Processing*, vol. 58, no. 3, pp. 1035–1048, March 2010.
- [19] J. Chen and A. H. Sayed, "Diffusion adaptation strategies for distributed optimization and learning over networks," *IEEE Transactions on Signal Processing*, vol. 60, no. 8, pp. 4289–4305, August 2012.
- [20] J. Chen and A. H. Sayed, "Distributed Pareto optimization via diffusion strategies," *IEEE Journal of Selected Topics in Signal Processing*, vol. 7, no. 2, pp. 205–220, April 2013.
- [21] R. Abdolee, B. Champagne, and A. H. Sayed, "Estimation of space-time varying parameters using a diffusion LMS algorithm," *IEEE Transactions on Signal Processing*, vol. 62, no. 2, pp. 403–418, Jan. 2014.

- [22] N. Bogdanović, J. Plata-Chaves, and K. Berberidis, “Distributed diffusion-based LMS for node-specific parameter estimation over adaptive networks,” in *Proc. IEEE International Conference on Acoustics, Speech and Signal Processing (ICASSP)*, Florence, Italy, May 2014, pp. 7223–7227.
- [23] J. Chen, C. Richard, A. O. Hero, and A. H. Sayed, “Diffusion LMS for multitask problems with overlapping hypothesis subspaces,” in *Proc. IEEE International Workshop on Machine Learning for Signal Processing (MLSP)*, 2014.
- [24] A. Bertrand and M. Moonen, “Distributed adaptive node-specific signal estimation in fully connected sensor networks – Part I: sequential node updating,” *IEEE Transactions on Signal Processing*, vol. 58, no. 10, pp. 5277–5291, Oct. 2010.
- [25] A. Bertrand and M. Moonen, “Distributed adaptive estimation of node-specific signals in wireless sensor networks with a tree topology,” *IEEE Transactions on Signal Processing*, vol. 59, no. 5, pp. 2196–2210, May 2011.
- [26] J. Chen, C. Richard, and A. H. Sayed, “Multitask diffusion adaptation over networks,” *IEEE Transactions on Signal Processing*, vol. 62, no. 16, pp. 4129–4144, August 2014.
- [27] J. N. Tsitsiklis, D. P. Bertsekas, and M. Athans, “Distributed asynchronous deterministic and stochastic gradient optimization algorithms,” *IEEE Transactions on Automatic Control*, vol. 31, no. 9, pp. 803–812, 1986.
- [28] S. Boyd, A. Ghosh, B. Prabhakar, and D. Shah, “Randomized gossip algorithms,” *IEEE Transactions on Information Theory*, vol. 52, no. 6, pp. 2508–2530, 2006.
- [29] S. Kar and J. M. F. Moura, “Convergence rate analysis of distributed gossip (linear parameter) estimation: Fundamental limits and tradeoffs,” *IEEE Journal of Selected Topics in Signal Processing*, vol. 5, no. 4, pp. 674–690, 2011.
- [30] S. Kar and J.M.F. Moura, “Sensor networks with random links: Topology design for distributed consensus,” *IEEE Transactions on Signal Processing*, vol. 56, no. 7, pp. 3315–3326, 2008.
- [31] T. C. Aysal, M. E. Yildiz, A. D. Sarwate, and A. Scaglione, “Broadcast gossip algorithms for consensus,” *IEEE Transactions on Signal Processing*, vol. 57, no. 7, pp. 2748–2761, 2009.
- [32] S. Kar and J. M. F. Moura, “Distributed consensus algorithms in sensor networks: Quantized data and random link failures,” *IEEE Transactions on Signal Processing*, vol. 58, no. 3, pp. 1383–1400, 2010.
- [33] D. Jakovetic, J. Xavier, and J. M. F. Moura, “Weight optimization for consensus algorithms with correlated switching topology,” *IEEE Transactions on Signal Processing*, vol. 58, no. 7, pp. 3788–3801, 2010.
- [34] D. Jakovetic, J. Xavier, and J. M. F. Moura, “Cooperative convex optimization in networked systems: Augmented Lagrangian algorithms with directed gossip communication,” *IEEE Transactions on Signal Processing*, vol. 59, no. 8, pp. 3889–3902, 2011.
- [35] X. Zhao and A. H. Sayed, “Asynchronous adaptation and learning over networks-Part I: Modeling and stability analysis,” to appear in *IEEE Transactions on Signal Processing*. Also available as arXiv:1312.5434, December 2013.
- [36] X. Zhao and A. H. Sayed, “Asynchronous adaptation and learning over networks-Part II: Performance analysis,” to appear in *IEEE Transactions on Signal Processing*. Also available as arXiv:1312.5438, December 2013.
- [37] X. Zhao and A. H. Sayed, “Asynchronous adaptation and learning over networks-Part III: Comparison analysis,” to appear in *IEEE Transactions on Signal Processing*. Also available as arXiv:1312.5439, December 2013.
- [38] L. Grady and J. R. Polimeni, *Discrete Calculus: Applied Analysis on Graphs for Computational Science*, Springer, 2010.
- [39] T. Basar and G. J. Olsder, *Dynamic Noncooperative Game Theory*, London, Academic Press, 2nd edition edition, 1995.
- [40] J. B. Rosen, “Existence and uniqueness of equilibrium points for concave n-person games,” *Econometrica: Journal of the Econometric Society*, vol. 33, no. 3, pp. 520–534, 1965.
- [41] A. H. Sayed, *Adaptive Filters*, John Wiley & Sons, NJ, 2008.
- [42] R. H. Koning, H. Neudecker, and T. Wansbeek, “Block Kronecker products and the vecb operator,” *Linear Algebra and its Applications*, vol. 149, pp. 165–184, April 1991.
- [43] R. A. Horn and C. R. Johnson, *Matrix Analysis*, Cambridge University Press, 2003.
- [44] J. Mitola and J.Q. Maguire, “Cognitive radio: making software radios more personal,” *Personal Communications, IEEE*, vol. 6, no. 4, pp. 13–18, August 1999.

- [45] P. Di Lorenzo, S. Barbarossa, and A. H. Sayed, "Bio-inspired decentralized radio access based on swarming mechanisms over adaptive networks," *IEEE Transactions on Signal Processing*, vol. 61, no. 12, pp. 3183–3197, June 2013.
- [46] D. S. Bernstein, *Matrix Mathematics: Theory, Facts, and Formulas with Application to Linear Systems Theory*, Princeton University Press, 2005.